Development of an isotope dilution technique for the quantitative analysis of fission gases in nuclear fuels

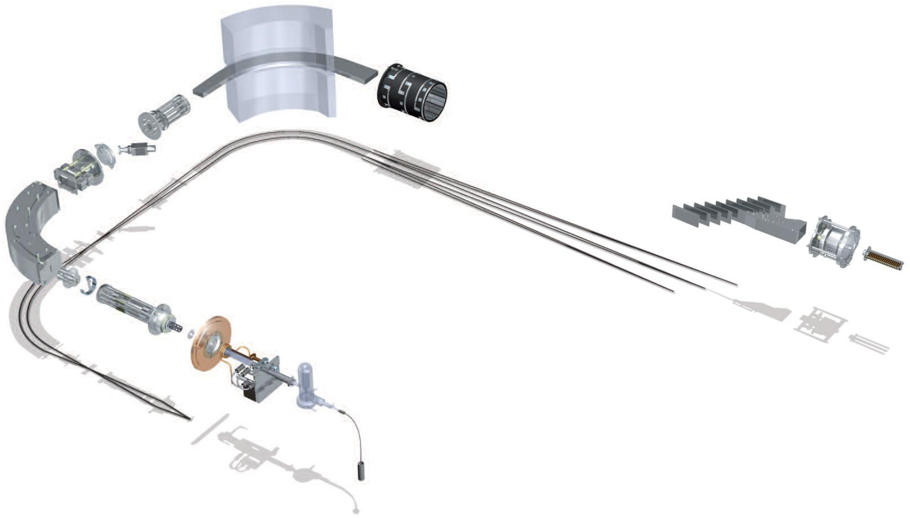

Master Thesis WS 09/10
Department of Nuclear Energy and Safety (NES)
AHL – Isotope and Elemental Analysis

Author: Claudio Feliciani

Advisor: Niko Kivel
Supervisor: Ines Günther-Leopold
Tutor: Prof. Rakesh Chawla

For my parents and my sister
who wonder what I do all day

Contents

List of Figures

List of Tables

Nomenclature

Abbreviations

COM	Component Object Model
DF	Dilution Factor
EI	Electron Impact
EL	Extraction Lens
ESA	Electrostatic Analyzer
FBR	Fast Breeder Reactor
FGR	Fission Gas Release
FP	Fission Product
FS	Full Scale
HFR	High Flux Reactor
GB	Grain Boundary
$GSMS$	Gas Source Mass Spectrometry
GUM	Guide to the Expression of Uncertainty in Measurement
ICP	Inductively Coupled Plasma
$IDMS$	Isotope Dilution Mass Spectrometry
ISO	International Organization of Standardization
IT	Isomeric Transition
LA	Laser Ablation
LWR	Light Water Reactor
MDD	Mixing and Diluting Device
MS	Mass Spectrometry
MOX	Mixed Oxide
MC	Multi Collector
ND	Not Determined

NPP	Nuclear Power Plant
NI	National Instruments
PCI	Pellet-Cladding Interaction
ppm	parts per million
PWR	Pressurized Water Reactor
RF	Radio Frequency
RS	Recommended Standard
STD	Standard Deviation
$SIMS$	Secondary Ion Mass Spectrometry
TOF	Time Of Flight
TTL	Transistor-Transistor Logic
USB	Universal Serial Bus
VCR	Vacuum Coupling Radiation
VI	Virtual Instrumentation
XS	Cross Section

Roman

A	Abundance	[%]
c	Concentration	$[\frac{\mathrm{mol}}{\mathrm{L}}]$
C	Concentration	[-]
D	Diffusion coefficient	$[\frac{\mathrm{cm}^2}{\mathrm{s}}]$
m	Mass	[kg]
M	Relative molecular weight	$[\frac{\mathrm{g}}{\mathrm{mol}}]$
n	Amount of substance	[mol]
N	Number of atoms	[-]
p	Pressure	[bar]
R	Isotope ratio	[-]
T	Temperature	[K]
V	Volume	$[\mathrm{m}^3]$
Z	Atomic number	[-]

Subscript

B	Blend
tot	Total
X	Sample
Y	Spike

Greek

ω	Angular frequency	$[\frac{\text{rad}}{\text{s}}]$
σ	Collision diameter	[Å]
σ	Relative uncertainty	[%]
Ω	Collision integral	[-]
ϵ	Energy of interaction	[J]

Constants

k_B	Boltzmann constant	$[\frac{\text{m}^2\text{kg}}{\text{s}^{-2}\text{K}}]$
N_A	Avogradro's number	$[\text{mol}^{-1}]$
R	Ideal gas constant	$[\frac{\text{J}}{\text{mol K}}]$

Abstract

For about one quarter of the fissions in nuclear fuel, one of the two formed fission products is gaseous. Xe and Kr, because of their very low solubility in the fuel matrix, they accumulate in the fuel and are later released in the plenum. These noble gases deteriorate the mechanical properties of the fuel and increase the pressure in the plenum. In addition, the isotope ^{135}Xe *has a crucial importance on the neutronical behavior of the reactor because of its large neutron capture cross section.*
The knowledge of the composition of the fission gas in both the plenum and the fuel matrix represents a milestone for the understanding of the phenomena related to fission gas release and thus is of particular importance for safety assessment studies.
To increase the capability of the fuel to retain fission gases, the use of additives to nuclear fuel is under investigation. Because of these developments, in the future, a reduced concentration of Xe and Kr in the plenum is envisaged.

Elemental and isotopic composition of fission gases are routinely measured in PSI's Hot Laboratory using GSMS. With this device only Xe concentrations greater than about 1% (n/n) can be measured. Below this limit measurements become unreliable.

To confirm independently the results of GSMS and allow measuring low Xe concentrations in fission gases a method based on IDMS has been developed in the frame of this study. For this scope a device has been built in order to dilute fission gas by mixing it with Ar for the direct measurement with MC-ICP-MS. A central part of this work has been the optimization of the mixing-diluting device aiming to obtain homogeneous gas mixtures. Different designs, geometries and dilution methods have been investigated to reach an adequate mixture quality. Fission gases produced in different fuel rods have been finally measured applying the IDMS method using MC-ICP-MS. The results have been compared with the ones obtained by GSMS for the same gas samples.

Part I

Introduction and fundamentals

Chapter 1

Introduction

1.1 Nuclear fuel

In nuclear reactors fuel is inserted by means of complex structures which confine it and avoid that fission products can escape in the cooling system. Fuel itself is contained in fuel pellets, composed by UO_2 powder, which has been pressed and sintered. Being a ceramic material the uranium dioxide has the advantage of melting at high temperature and can maintain the same geometry under irradiation conditions. To allow the use in commercial power reactors the amount of fissionable isotopes ($^{235}U/U_{total}$ for uranium fuel) is often enriched from the natural composition of 0.72% (n/n) to a concentration of 3–5% (n/n).

Fuel pellets are filled into cladding tubes (fuel rod), applying a certain pressure of He. In Light Water Reactors (LWR) several fuel rods are then combined in square structures and kept at a given distance to allow an optimal heat removal. Fuel assemblies are 3–4 meters long and their active part compose the core of the reactor. A typical fuel assembly for commercial power plants can contain between 100 and 150 fuel rods, and up to 150 fuel assemblies can be used in a reactor depending on the configuration. A power reactor can contain several tons of heavy metal, which allow to reach power in the order of some GW of electric power.

In modern reactors UO_2 is often used in combination with Pu which is normally obtained by reprocessing spent fuel. This type of fuel configuration is called mixed oxide (MOX). Depending on the design of the reactor up to 50% of the core can be filled with this type of fuel.

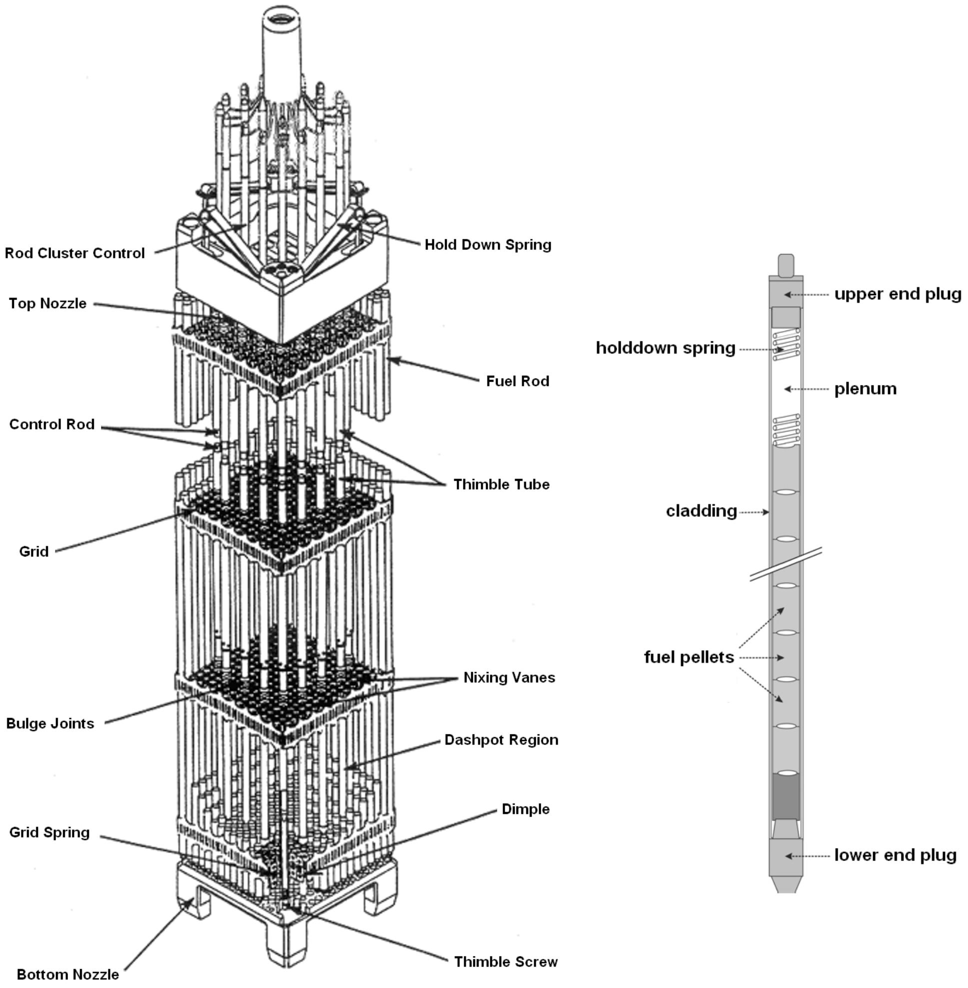

(d) Fuel assembly [1]. (e) Fuel rod [1].

Figure 1.1: Fuel structure in nuclear power reactors (PWR).

1.2 Nuclear fission

Nuclear power is produced by fission reactions occurring within the core of nuclear reactors. The fission of one heavy nucleus results in two fission fragments that recede from each other with a kinetic energy of about 175 MeV and in 2–3 neutrons (on average 2.43 for ^{235}U) with a total energy of about 5 MeV which gives the basis for the chain reaction (see Table 1.1).
With the delayed process of fission fragment decay, the usable energy sums up to 200 MeV, i.e. one single fission produces 3.2010^{-11} J of energy, which means many thousand times more energy is released by fission than in a chemical reaction. Fission can be subdivided into two types: the spontaneous and the induced fission. Spontaneous fission, a form of radioactive decay, occurs randomly without external

trigger, while induced fission is triggered by a neutron with an appropriate energy so that the nucleus can capture this neutron.

Table 1.1: Fission reaction energy distribution [2].

Kinetic energy of fission products	175 MeV	Prompt heat
Kinetic energy of fission neutrons	5 MeV	Prompt heat
Prompt γ radiation	7 MeV	Prompt heat
Fission products $\gamma + \beta^+$ radiation	7 + 6 MeV	Decay heat
Neutrinos	10 MeV	

This ability to capture depends on the cross section of the fissile nucleus. After the neutron capture, the nucleus turns unstable and decays to fission fragments and kinetic energy. Candidates for energy production from fission are ^{232}Th, ^{233}U, ^{235}U, ^{238}U, and ^{239}Pu with large cross sections for thermal neutrons (eV range) or fast neutrons (MeV range). The commonly used nuclear fuels in western modern power plants are enriched in ^{235}U and ^{239}Pu as fissile nuclide in form of ceramic (oxide) pellets.

The fission products (FP) of one fission have normally unequal masses. The most probable masses in ^{235}U fuel are 135 for the heavy and 95 for the light FP, respectively (see Figure 1.2 and Table 1.2).

Table 1.2: ^{233}U and ^{235}U cumulative thermal fission yield (list is not complete) [3].

Isotope	^{233}U	^{235}U	Half-life
^{135}Xe	5.47 %	6.61 %	9.14 h
^{133}Xe	5.98 %	6.60 %	5.24 d
^{133}I	5.94 %	6.59 %	20.87 h
^{95}Zr	6.38 %	6.50 %	64.03 d
^{95}Nb	6.38 %	6.49 %	34.99 d
^{135}I	4.31 %	6.39 %	6.57 h
^{140}La	6.45 %	6.31 %	1.68 d
^{140}Ba	6.43 %	6.31 %	12.57 d
^{137}Cs	6.20 %	6.22 %	30.05 y
^{99}Tc	5.03 %	6.13 %	2.11 y
^{99}Mo	5.03 %	6.13 %	stable
^{141}Ce	6.21 %	5.86 %	32.51 d
^{90}Sr	6.64 %	5.73 %	28.8 y
^{144}Nd	4.65 %	5.47 %	stable
^{144}Ce	4.65 %	5.47 %	285.1 d
^{144}Pr	4.65 %	5.47 %	17.28 min
⋮	⋮	⋮	⋮

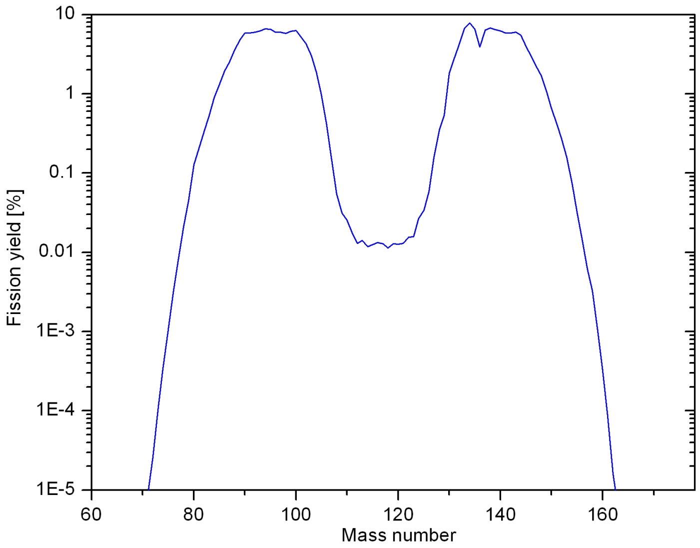

Figure 1.2: ^{235}U cumulative thermal fission yield [4].

Detectable amounts of fission product yields are in the mass range of 72–166. Noble fission gases require special attention as they do not combine with other species. They have low solubility in a UO_2 matrix and remain in gaseous phase.

Table 1.3: Cumulative fission yields (in %) of the noble gases from the fission of different nuclides with thermal neutrons [3] [5] [6].

Isotope ($t_{1/2}$)	^{233}U	^{235}U	^{239}Pu	Isotope ($t_{1/2}$)	^{233}U	^{235}U	^{239}Pu
^{83}Kr (stable)	1.03	0.53	0.29	^{131}Xe (stable)	3.52	3.00	3.78
^{84}Kr (stable)	1.89	0.99	0.48	^{132}Xe (stable)	4.77	4.38	5.26
^{85}Kr (10.8 y)	0.51	0.28	0.12	^{133}Xe (5.24 d)	5.95	6.60	6.92
^{86}Kr (stable)	3.17	1.98	0.77	^{134}Xe (stable)	6.11	7.70	7.21
				^{135}Xe (9.14 h)	5.90	6.61	7.18
				^{136}Xe (stable)	7.04	6.29	6.63
Total Kr	6.60	3.78	1.66	Total Xe	33.29	34.58	36.98

In UO_2 or MOX fuel roughly 35% of the FP are gaseous (see Table 1.3), mainly Kr and Xe isotopes. It has been reported that the Kr : Xe ratio for the ^{235}U fission is 1 : 5.7 and for the ^{239}Pu 1 : 14 [7]. At higher burnup, the ratio of the fissions from ^{235}U to ^{239}Pu is around 3 : 1. Therefore, the total noble gas fission yield leads to 3.3% for Kr, and 22.2% for Xe and the Kr : Xe ratio results in 1 : 6.7.

Chapter 2

Fission gases

2.1 Introduction

The problems related to the release of fission gases within nuclear fuel are of major concern in different fields of nuclear research. Firstly, this topic is treated in material science, since the deposition of noble gases within the fuel strongly influences the capability of it to withstand high temperatures and mechanical stresses. Moreover since some isotopes of noble gases (like ^{135}Xe) have a large neutron capture cross-section the knowledge of the mechanisms of fission gas release can be used to increase the accuracy of neutronical studies. Because of fuel's swelling caused by fission gas production and the increased amount of the same within the gap between pellet and cladding, the heat conductivity of the fuel element will change with the burnup. Thus thermal hydraulic studies have to consider the influence of fission gases when creating a model to simulate the heat exchange process between fuel and coolant.

Fission gas behavior

Xe and Kr comprise approximately 35% of the fission products. They are chemically inert to (and insoluble in) UO_2 and MOX fuel matrix. Thus, the gases tend to precipitate as bubbles (causing swelling) and to diffuse to free surfaces (leading to internal pressurization of fuel elements). The amount of gas released depends on the operating conditions and the design of both reactor and fuel. For example, because of modest power ratings, fuel in a LWR core can retain up to 95% [8] and more of its gas at temperatures where gas swelling is low. This allows high burnup with minimal pellet-cladding interaction (PCI) and with no tendency to overpressurize the limited free space available in rods. But PCI will also be increased because of the sudden swelling and release of retained gas. This vulnerability of LWR fuel has led to extensive investigation of the phenomena with a particular

emphasis on modeling fission gas release (FGR) with computer codes in order to predict fuel element performance.
Although driven by the same phenomena as LWR fuel, due to high power ratings fast breeder reactor (FBR) fuel retains only 10–20% [8] of fission gas during normal reactor operation. Thus fuel elements are designed on the assumption of 100% release. FBR fuel exhibits minimal PCI and a wide margin to failure under upset conditions.

2.2 Mechanisms of fission gas release

FGR is related to different mechanisms. The understanding of the combination of these mechanisms with the physical processes and variables involved can help to create a model able to calculate the amount of fission gas produced and its rate of production. The understanding of where and in which form noble gases are retained within the fuel matrix is crucial.
The most important mechanisms related to FGR are:

1. recoil and knock-out
2. lattice diffusion
3. trapping
4. irradiation induced resolution
5. thermal diffusion
6. bubble interlinkage

The ensemble of mechanisms listed above depends on physical variables which can be either related to the operating conditions of the reactor or the structure and the composition of the fuel. The most important are temperature and fission rate (which are both related to the reactor power), burnup, fuel and gas properties (like diffusion coefficients of gases within the fuel matrix). The fuel microstructure, grain size, cracking properties, dislocation size and position are other physical variables capable of influencing the phenomena related to FGR.

2.2.1 Recoil and knock-out

Recoil

As a result of the fission reaction a fissile isotope is split into two atoms with an energy of about 80 MeV. In UO_2 fuel the distance that such a fission fragment needs to travel to rest is about 10 μm. When it stops it becomes an impurity atom in the lattice. Along the path traveled by these fragments, point defects are left which can be filled by fission gases. This athermal process only affects the outer fuel layer and thus its occurring probability is proportional to the geometric surface to volume ratio.

Knock-out

Close to the fuel surface a gas atom can be knocked out directly into the plenum by fission fragment or fission spike interaction. Since this phenomenon only occurs at the surface (the range of knocked atoms is about 20 nm), its influence on FGR will be proportional to the total surface to volume ratio. Like for the recoil mechanism, knock-out is athermal, since it only considers collision resulting from a nuclear reaction.

2.2.2 Lattice diffusion

Since the fuel itself is in the form of oxide, the fission reaction can be considered as an oxidation process for the fuel, because of the Oxygen release during the nuclear reaction. This Oxygen usually combines with fission products (like in the case of Cesium) or remains in solution making the fuel hyperstoichiometric. Inert fission gases (Xe and Kr), however, can neither combine with Oxygen nor with other elements in the fuel, thus remaining within the matrix as precipitates. At normal temperatures this would result in a homogeneous distribution of inert gases within the fuel pellet. However, nuclear fuel reaches temperatures in the order of 1000°C during operation. At these temperatures the lattice diffusion coefficient becomes large and gas atoms can easily move inside the fuel. Although temperature has the biggest influence on lattice diffusion, its coefficient can be influenced by other physical variables, the most important being: stoichiometry of the fuel (enhanced diffusion), additives, burnup and fission rate. Correlations to calculate the lattice diffusion coefficient are available in the literature (for example the Turnbell's equation) and can estimate its value with good accuracy.

2.2.3 Trapping

Trapping in grains

Because of their low solubility (for Xe about 0.3% (m/m)), noble gases can be trapped in as-fabricated defects or induced ones. As-fabricated defects can be of different types: impurities, small pores or dislocations, while radiation induced ones include: vacancy clusters, fission gas atoms and bubbles and precipitates of solid fission products. Figure 2.1 shows an electron microscope image of intergranular bubbles.

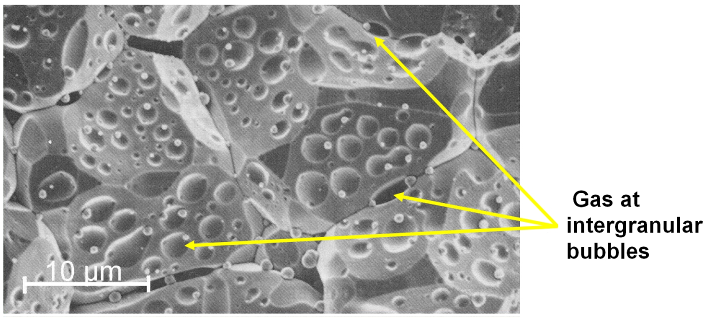

Figure 2.1: Intergranular bubbles [1].

Trapping in grain boundaries

Grain boundaries represent a sink for fission products. The accumulation of gas in these regions results in large bubbles (μm size) which can interconnect each other leading to even bigger bubbles. The amount of gas accumulating at grain boundaries is not homogeneous within the fuel pellet and might depend on local charges, dipolar moments and the local stoichiometry.
Both trapping mechanisms increase with fission density, gas concentration and burnup. Trapping already occurs at low burnup. Figure 2.2 shows an electron microscope image of bubbles trapped at grain boundaries.

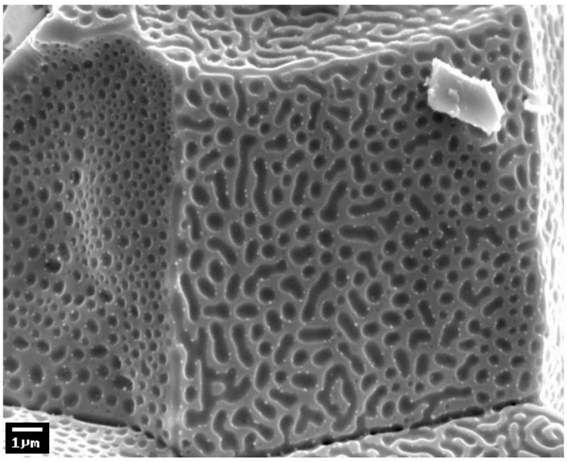

Figure 2.2: Bubbles at grain boundaries [1].

2.2.4 Irradiation induced resolution

Bubbles grow by absorbing vacancies and gas-atoms. This growth is however limited by one phenomenon. Bubbles can be dispersed in case of direct collision with fission fragments or interaction with the heat affected zones produced by ionization around the trajectories of other fission fragments. This phenomenon is known as irradiation induced resolution (or simply "resolution"). Its occurrence causes a dynamic solubility of fission gas in the lattice and can avoid the formation of large bubbles.

2.2.5 Thermal diffusion

In the presence of a temperature gradient, fission products, Uranium and Oxygen migrate in different directions in the fuel, corresponding to hot or cold regions (Soret effect). As a result of this phenomenon actinides, Oxygen and noble gases are redistributed in the fuel matrix.

2.2.6 Bubble interlinkage

Once the bubbles at the grain boundaries (GBs) have reached a critical size, they can interconnect and ultimately form open tunnel networks which drives the release of gas from the fuel. The interlinkage mechanism can explain the incubation time needed for the release and the burst release observed during abrupt power excursion. In UO_2 fuel at low burnup and power densities the gas content of the bubbles is about 20% of the total gas generated up to 1300°C and a maximum of about 40% at 1600°C [9].

2.3 Other important aspects on FGR

Rate of gas production

The fission rate, although being proportional to the reactor power, is not constant within the fuel pellet. What is usually observed is that at the centerline the power density is higher than at the outer fuel, resulting in a larger FGR at the center of the pellet than at its boundary. The combination of the mechanisms described in the previous section leads to a different swelling distribution respect to the one which could be obtained by only considering the production rate of noble gases. In fact although the production has its peak in the center, the accumulation (and the swelling) are maximal in the region between the centerline and the outer fuel. Table 2.1 gives a summary of the local effects of FGR within fuel pellets.

Table 2.1: Gas release within the pellet.

Centerline	Middle	Outer fuel
Large release	Medium release	Low release
Low swelling	Large swelling	Low swelling

2.4 The role of Xe in fission gas

2.4.1 Xe in nature

Xe is a noble gas normally found in trace amounts (0.0087 parts per million (ppm) (m/v) [10]) in the air. Naturally occurring Xe consists of nine stable isotopes. Another 40 unstable isotopes undergo radioactive decay. Xe is colorless and odorless and, apart few exceptions, is generally inert. The natural isotopes of Xe and their atomic relative masses and mole fractions are listed in Table 2.2.

Table 2.2: Isotopic composition of natural occurring Xe [11].

Isotope	Atomic relative mass	Mole fraction
^{124}Xe	123.9058954(21)	0.000952(3)
^{126}Xe	125.904268(7)	0.000890(2)
^{128}Xe	127.9035305(15)	0.019102(8)
^{129}Xe	128.9047799(9)	0.264006(82)
^{130}Xe	129.9035089(11)	0.040710(13)
^{131}Xe	130.9050828(18)	0.212324(30)
^{132}Xe	131.9041546(15)	0.269086(33)
^{134}Xe	133.9053945(9)	0.104357(21)
^{136}Xe	135.907220(8)	0.088573(44)

In nature ^{129}Xe is only produced by beta decay of ^{129}I, which has a half-life of 16 million years, while ^{131m}Xe, ^{133}Xe, ^{133m}Xe, and ^{135}Xe are some of the fission products of both ^{235}U and ^{239}Pu, and therefore used as indicators of nuclear explosions.

2.4.2 Xe in nuclear reactors

Because fresh fuel elements are filled using He (to increase the pressure in the gap and enhance heat conduction from fuel to coolant), at zero burnup Xe is completely absent within the fuel element. With increasing burnup Xe becomes the main component of fission gas with concentrations of about 50% (n/n). Figure 2.3 shows the composition of the fission gas from a Swiss NPP for three fuel rods with different burnup.

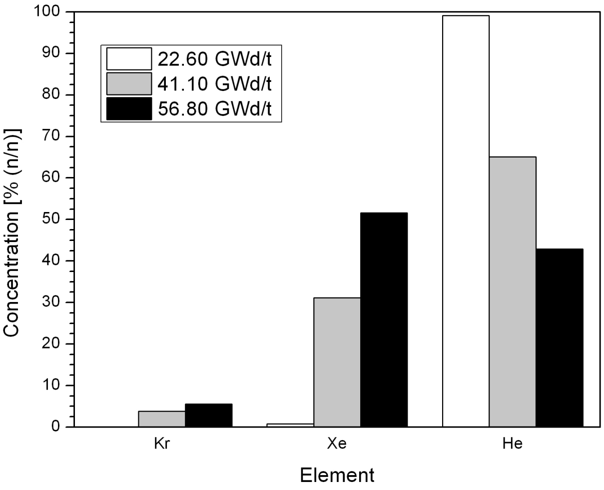

Figure 2.3: Fission gas composition [12].

Although being one of the main components of fission gas, Xe has relatively small independent fission yield (see table Table 2.3).

Table 2.3: Xe independent fission yields for ^{235}U fuel [3].

Isotope	Thermal fission yield [% per fission]	Fast fission yield [% per fission]	Half-lives	Decay-mode
^{128}Xe	0	0	Stable	-
^{130}Xe	$4.80 \cdot 10^{-9}$	$9.30 \cdot 10^{-9}$	Stable	-
^{131m}Xe	$3.60 \cdot 10^{-7}$	$7.40 \cdot 10^{-7}$	11.930 d	IT
^{133}Xe	0.00044	0.00071	5.243 d	β^-
^{133m}Xe	0.00106	0.00198	2.19 d	IT
^{135}Xe	0.069	0.084	9.14 h	β^-
^{135m}Xe	0.167	0.236	15.29 min	β^- / 0.003 IT / 0.997

In fact Xe production in nuclear reactors is mostly caused by the decay of other fission products (like Cs and I) or by electron capture of the same. As a result of these reaction the isotopic composition of fission Xe is very different to the one found in nature. ^{129}Xe, which is the second most abundant isotope in nature, cannot be found in fission gases. Likewise ^{124}Xe and ^{126}Xe are completely absent from fission gases. On the other hand heavy isotopes (^{134}Xe – ^{136}Xe) are abundant in nuclear fuels in higher concentrations compared to natural Xe. This can be explained by considering that Xe can easily undergo neutron capture reactions, thus increasing its mass. This particularly applies to ^{135}Xe, which is absent from fission gas because of its very large neutron capture cross section (XS) and its short half-life ($t_{1/2} = 9.14$ h). Once a neutron has been absorbed, ^{135}Xe transforms in

^{136}Xe, which, in fact, is the main component of fission Xe.

The Xe isotopic composition changes only slightly with increasing burnup. The main trends are an increase in the concentration of ^{132}Xe and a decrease in ^{131}Xe. ^{134}Xe and ^{136}Xe isotopic abundances remain almost stable. Figure 2.4 gives an overview on the Xe isotopic composition in the fission gas from fuel pins of a Swiss NPP for three different burnups.

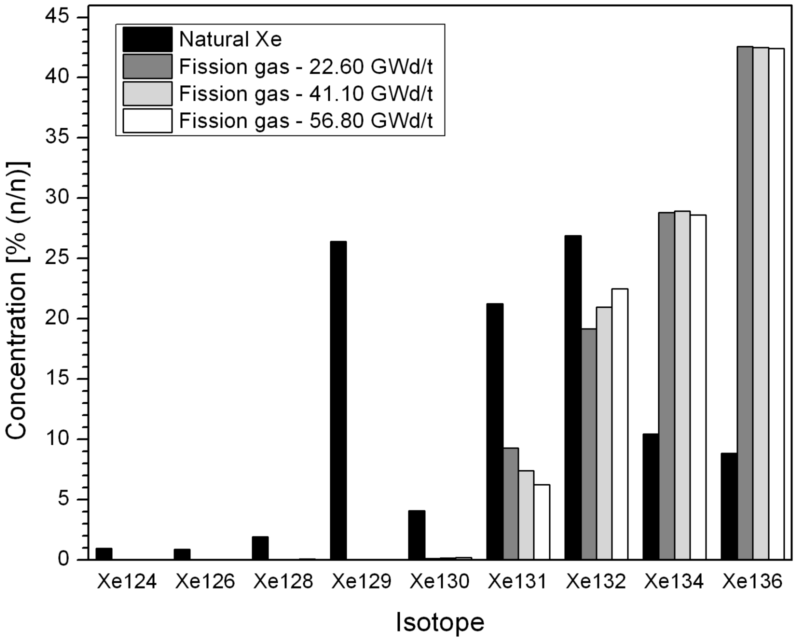

Figure 2.4: Xe isotopic composition in fission gas [12].

2.4.3 Xe poisoning and Xe transients

In nuclear reactors strong neutron absorbers (poisons) are often used in fresh fuel to compensate the high reactivity. In addition to artificially added poisons, isotopes with very large neutron capture cross sections are created during operation. Most of the Xe isotopes produced in nuclear reactors have a relatively small neutron capture cross section (Table 2.4).

This is not the case for ^{135}Xe, which has a thermal capture cross section of 2.6 millions barns (Figure 2.5). It is created by β^--decay of ^{135}I ($t_{1/2}$ = 6.57 h) and successive isomeric transition to stable state ($t_{1/2}$ = 15.29 min). During normal operation ^{135}Xe is kept at a constant concentration within the fuel, since the amount decayed from ^{135}I is rapidly converted into ^{136}Xe by neutron capture. However, as soon as the reactor is shut down the number of neutrons in the reactor will rapidly drop down, while the accumulated ^{135}I will continue to decay producing ^{135}Xe. Thus in the hours following the reactor shut-down the amount of ^{135}Xe in the fuel will rapidly increase to reach a maximum within a couple of hours. With high concentration of this strong neutron absorber the reactor cannot be restarted soon, since the reactivity margin would be dangerously exceeded. The reaction can be restarted only when the amount of ^{135}Xe has been naturally reduced by β^--decay into ^{135}Cs ($t_{1/2} = 9.14$ h) and by neutron capture. This can take several hours.

Table 2.4: Neutron capture cross sections for major Xe isotopes [13] in barns.

Isotope	Neutron capture XS (0.025 eV)	Neutron capture XS (1 MeV)
^{124}Xe	165.65	0.10916
^{126}Xe	2.22	0.06619
^{128}Xe	5.40	0.05630
^{129}Xe	18.13	0.08490
^{130}Xe	6.24	0.04753
^{131}Xe	90.66	0.02596
^{132}Xe	0.44	0.02591
^{133}Xe	191.35	0.00905
^{134}Xe	0.25	0.01435
^{135}Xe	2657782	0.00054
^{136}Xe	0.16	0.00179

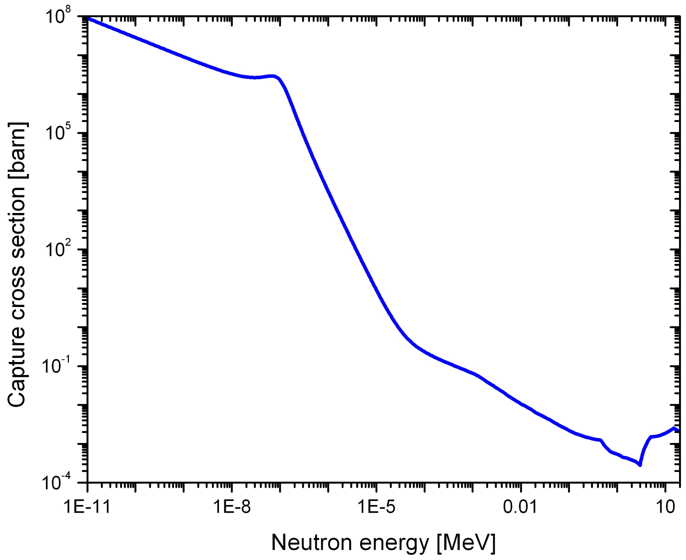

Figure 2.5: Neutron capture cross section of ^{135}Xe [13].

The underestimation of Xe transient effects is believed to be one of the major causes of the accident of Chernobyl. For this reason neutronical codes are now used to estimate the concentration of ^{135}Xe during different operating conditions in power reactors.

2.5 Analysis of fission gases

Analysis of composition of the fission gas in the fuel microstructure and in the plenum are typically performed using different methods.

Concerning the gas in the plenum, a gas source mass spectrometer (GSMS – see 6.2) is used to determine elemental and isotopic composition of the sample. Before starting the measurement of fission gas with GSMS a calibration gas with different isotopic but similar elemental composition compared to the fission gas is used to calibrate the response of the device. Later, when the device is calibrated, another calibration gas, different from the one used to calibrate the device, is measured as a "sample" to check the correct functioning of the equipment. Finally, if the concentrations measured for the calibration gas used as a "sample" are in good agreement with the certified values, fission gas composition is measured.

GSMS allows to detect all the elements in the fission gases, from the light ^{4}He up to the heavy ^{136}Xe and to distinguish each isotope for every component of the gas. Detection limits for modern GSMS are some ppm.

Analysis of the gas in the microstructure is mainly performed using secondary ion mass spectrometry (SIMS) and laser ablation inductively coupled plasma mass spectrometry (LA-ICP-MS) [14]. SIMS allows to analyze single atomic layer of the surface and has very low detection limits, often in ppm or ppb range. In LA-ICP-MS solid samples are exposed to a high energetic laser source leading to an ablation and the formation of aerosol. This aerosol is send to the ICP-MS for composition quantification. ICP-MS has low detection limits in the range of ppb.

Chapter 3

Isotope Dilution Mass Spectrometry (IDMS)

The technique of isotope dilution mass spectrometry (IDMS) was initially developed during the 1950s for elemental analysis [15]. Today it is widely used especially for liquid samples in both organic and inorganic chemistry. IDMS can be extended to solid samples if they can be dissolved in acid solutions. An application to gas samples has been never reported.

3.1 Isotope ratios

Relative isotopic abundances cannot be measured directly. An isotope ratio (R) for a specific element in a sample is, however, experimentally accessible. An isotope ratio is defined as:

$$R = \frac{n(^{i}E)}{n(^{j}E)} \tag{3.1}$$

where E refers to a specific element and n represents the amount of isotope i and j. By using mass spectrometry the amount of a given isotope in a sample is measured as an electric current, thus Equation 3.1 can be rewritten as:

$$R \approx \frac{I(^{i}E)}{I(^{j}E)} \tag{3.2}$$

An isotope ratio is a very robust quantity as the number of parameters which influence it are limited and their effect is generally quite small. There are some mass-dependent processes, however, which cause a small, but measurable bias due to the difference in mass between the isotopes measured. This difference is known under the general concept of mass bias (or mass discrimination). Thus mass bias corrected values can be obtained as a final output of MS measurements.

Ratios obtained with modern MS easily reach a relative uncertainty of less than

0.1% and represent therefore a robust basis for the results which can be obtained applying isotopic dilution techniques.

3.2 Principle of IDMS

The basic idea of IDMS is that by introducing a deliberate change in a chosen isotope ratio of an element, it is possible to determine the amount or the concentration of this element in the sample studied. For this purpose, a known amount of an isotopically enriched element is added to the sample (the spiking process). It is important to choose a spike with an isotopic composition significantly different from the one in the sample. A schematic of the IDMS concept is illustrated in Figure 3.1.

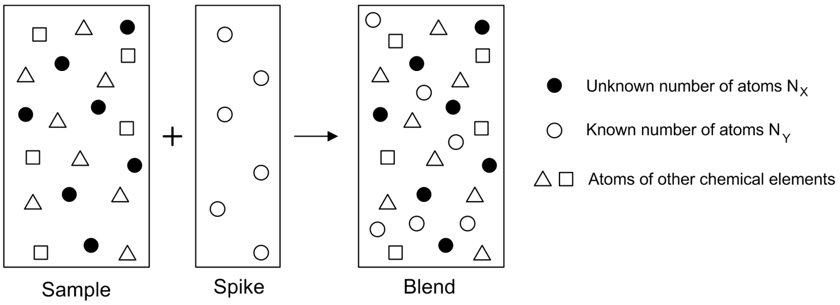

(a) Spike, sample and blend composition [16].

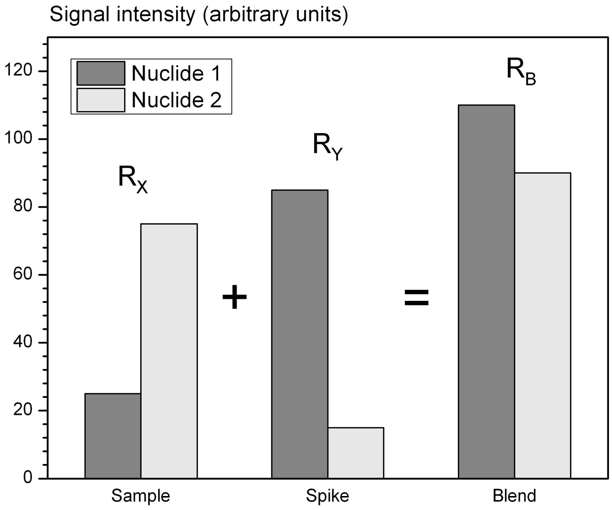

(b) Signal for spike, sample and blend [16].

Figure 3.1: Schematic representation of the principle of IDMS.

The most important stages in IDMS can be summarized as:

1. Characterization of the spike (isotopic analogue of the sample).

2. Addition of known amount of spike to a known amount of the sample (spiking process). This can be done as a batch process where the spike and the sample are mixed once gravimetrically or volumetrically or as an online process where spike and sample are delivered to the mass spectrometer at constant well known mass-flow rates.
3. Equilibration of the mixture (blend) for an appropriate time (in case of batch process).
4. Accurate measurement of the isotopic ratio of the blend using a mass spectrometer.

In the simple case, by taking only one isotope for both spike and sample, the blend ratio can be given as the ratio of the number of atoms in the spike to the number of atoms in the sample. This can be written as:

$$\frac{N_{\mathrm{X}}}{N_{\mathrm{Y}}} = R_{\mathrm{B}} \tag{3.3}$$

where subscript X has been used for the sample, Y for the spike and B for the blend. Thus if the amount of spike is known the quantity of sample can be calculated by measuring the blend isotope-ratio.

For the more general case, in which the elements have i different isotopes, the equation can be written as [15]:

$$\frac{N_{\mathrm{X}}}{N_{\mathrm{Y}}} = \frac{R_{\mathrm{Y}} - R_{\mathrm{B}}}{R_{\mathrm{B}} - R_{\mathrm{X}}} \frac{\sum_i (R_{\mathrm{X}})_i}{\sum_i (R_{\mathrm{Y}})_i} \tag{3.4}$$

where N is defined as the number of atoms and R is the isotope ratio, with a particular isotope selected as reference. Since $N = \mathrm{N_A} n$, $\mathrm{N_A}$ being the Avogadro's constant and n the amount of substance (in mol), Equation 3.4 can be rewritten as:

$$\frac{n_{\mathrm{X}}}{n_{\mathrm{Y}}} = \frac{c_{\mathrm{X}} m_{\mathrm{X}}}{c_{\mathrm{Y}} m_{\mathrm{Y}}} = \frac{R_{\mathrm{Y}} - R_{\mathrm{B}}}{R_{\mathrm{B}} - R_{\mathrm{X}}} \frac{\sum_i (R_{\mathrm{X}})_i}{\sum_i (R_{\mathrm{Y}})_i} \tag{3.5}$$

where c is the molar concentration in the solution. Thus the concentration of the sample can be calculated by rearranging Equation 3.5 as follows:

$$c_{\mathrm{X}} = c_{\mathrm{Y}} \frac{m_{\mathrm{Y}}}{m_{\mathrm{X}}} \frac{R_{\mathrm{Y}} - R_{\mathrm{B}}}{R_{\mathrm{B}} - R_{\mathrm{X}}} \frac{\sum_i (R_{\mathrm{X}})_i}{\sum_i (R_{\mathrm{Y}})_i} \tag{3.6}$$

3.3 Advantages and disadvantages of IDMS

3.3.1 Advantages of IDMS

One of the major advantages of IDMS is that it deals with isotope ratios instead of signal intensities. Because of the use of ratios many sources of error can be eliminated and the results are very robust against response changes during the measurements. Moreover the IDMS method for liquid samples is very easy to apply and, as for internal calibration, only few additional equipment is required. Lastly, losses of sample after the spiking process are unproblematic since isotope ratios remain unchanged.

3.3.2 Disadvantages of IDMS

In some cases suitable isotopic material has to be specifically created. Since some isotopes are available in limited amount and the operation of creating an isotopic mixture requires special devices, the costs can rapidly increase. Moreover for optimal results, IDMS requires multi collector MS. These are much more expensive than single collector machine and contribute in increasing the total cost of the experimental hardware necessary. Lastly, IDMS only works with elements having at least two isotopes.

3.4 IDMS applied to Xe

Xe has nine naturally occurring isotopes. The same number of isotopes, but in different proportion can be found in fission gas samples. The Neptune MC-ICP-MS (see Chapter 6.3.7) has nine detectors, which means that all isotopes of Xe can be simultaneously measured and very accurate isotope ratios are obtained.
In this study Ar-diluted fission gas is used as sample, while natural Xe diluted in Ar at 20 ppm (n/n) is used as spike. The concentration of the latter is certified with a relative uncertainty of 0.5%. A mixture of fission gas, natural Xe (both in small amount) and Ar (in large amount) is therefore the blend.
Being the main component in the spike (and abundant in the blend) $^{132}\mathrm{Xe}$ is used as reference isotope to measure the isotope ratios. Thus as a result of the measurements with MC-ICP-MS the following ratios are obtained for both spike and blend (sample ratios must be calculated):

$$R_{124} = \frac{^{124}\mathrm{Xe}}{^{132}\mathrm{Xe}} \quad R_{126} = \frac{^{126}\mathrm{Xe}}{^{132}\mathrm{Xe}} \quad R_{128} = \frac{^{128}\mathrm{Xe}}{^{132}\mathrm{Xe}} \quad R_{129} = \frac{^{129}\mathrm{Xe}}{^{132}\mathrm{Xe}}$$

$$R_{130} = \frac{^{130}\mathrm{Xe}}{^{132}\mathrm{Xe}} \quad R_{131} = \frac{^{131}\mathrm{Xe}}{^{132}\mathrm{Xe}} \quad R_{134} = \frac{^{134}\mathrm{Xe}}{^{132}\mathrm{Xe}} \quad R_{136} = \frac{^{136}\mathrm{Xe}}{^{132}\mathrm{Xe}}$$

The isotopic composition for spike and blend can be trivially obtained using:

$$A_j^{\mathrm{X/B}} = \frac{R_j^{\mathrm{X/B}}}{\sum_i R_i^{\mathrm{X/B}} + 1} \tag{3.7}$$

where A represents the abundance and j a specific isotope. In the case of the sample its isotopic composition cannot be directly obtained. In contrast to spike and blend the sample is never measured in a direct way, but only indirectly when mixed within the blend. However, its isotopic composition can be readily obtained applying the following equation:

$$A_j^{\mathrm{Y}} = \frac{\left(A_j^{\mathrm{B}} - \dfrac{A_{129}^{\mathrm{B}}}{A_{129}^{\mathrm{X}}} A_j^{\mathrm{X}}\right)}{\sum_i \left(A_i^{\mathrm{B}} - \dfrac{A_{129}^{\mathrm{B}}}{A_{129}^{\mathrm{X}}} A_i^{\mathrm{X}}\right)} \tag{3.8}$$

Here ^{129}Xe is used as a reference isotope being the second most abundant in natural Xe and completely absent in fission gas. With the calculated sample abundance, the previously unknown sample isotope ratios can be computed taking ^{132}Xe as a reference isotope . Finally, using the isotope ratios of spike and blend measured with MC-ICP-MS and the ones of the sample computed, the total concentration of Xe in the sample can be calculated using Equation 3.6.

Chapter 4

Motivation and aim of the study

4.1 Motivation

As discussed in Chapter 2 fission gases play a very important role in safety issues in nuclear engineering. Research is constantly undergoing to determine and understand the mechanisms related to phenomena such as fission gas release, fuel cracking or pellet-cladding interaction. Among other gases, Xe has a crucial importance due to its neutronical properties. For all these studies the knowledge of the amount of gas released and its composition represent an important milestone. The measurement of the composition of fission gases is routinely performed in PSI's Hot Laboratory using GSMS. This device is capable of measuring Xe concentrations higher than about 1% (n/n). This limit does not represent a problem if normal standard UO_2 or MOX fuel is analyzed. In fact for standard UO_2 or MOX fuel typical Xe concentrations range from about 10% (n/n) to 50% (n/n), depending on the burnup. However, experiments are undergoing to employ a new type of fuel capable of retaining a larger amount of fission gases in the fuel matrix, reducing the amount released in the plenum [17] [18]. The reduction of fission gas released is performed using additives such as Cr_2O_3 or Al_2O_3. It is to expect that in the future the fission gas in the plenum will have a very small concentration of Xe, especially at low burnup. To measure this reduced concentration a new type of analysis is required, capable of measuring below 1% (n/n) with high precision. Besides the need of detecting low Xe concentration for future fuel development, preliminary evaluations have been started to implement a GSMS in the high flux reactor (HFR) Petten in the Netherlands to perform online measurements of fission gases during operation [19] [20]. The concentrations of Xe released during operation will range in the ppm.

4.2 Aim of the study

Although GSMS has been used for more than 10 years to perform fission gas analysis, its accuracy could be never compared with other devices, being the only one in the Hot Laboratory able to perform measurements of the composition of the gas collected in the plenum. Thus, a first aim of the study is to perform the same type of measurements as GSMS using a completely independent method and device. This would allow a direct comparison of the results obtained with both devices.
The independent method applied at the scope of this study is the IDMS in combination with MC-ICP-MS. This experimental device has been chosen because of its capabilities, its high precision and the good results obtained in the past.
Ideally the precision of the Xe concentrations measured using the new developed method should be similar to the one obtained with GSMS. However, because of the high precision in measuring isotope ratios of MC-ICP-MS, precision of the Xe concentration could be even higher than the one obtained by GSMS.
The method developed should allow an online measurement in order to be applicable to the direct measurement of fission gases during reactor operation as discussed previously.

Part II

Experimental

Chapter 5

Fission gas extraction from irradiated fuel rods

The extraction of fission gas from irradiated fuel rods is performed at PSI's Hot Laboratory using a device specifically designed for this scope. At first, the fuel rod is inserted and blocked in the gas extraction platform. There, an hart-metal tip is pressed on the surface of the fuel rod using a rotating spindle [21]. When a hole is formed the fission gas flows from the plenum of the fuel rod to a previously evacuated known volume in the gas extraction device. During this operation the pressure in the gas extraction device is constantly displayed and recorded. When pressure equilibrium is reached gas sample cylinders (see Figure 5.1), with a volume of about 50 mL, can be filled for later measurements using MS.

Figure 5.1: Gas sample cylinder.

When enough gas sample cylinders have been filled, the system of gas extraction device and fuel rod can be completely evacuated using a turbomolecular pump to start measuring the volume of the fuel rod. This unknown volume is measured using cylinders with known volume filled with He at a given pressure. When a sufficient vacuum is reached one of these cylinders can be opened and the pressure is recorded. Using the known volume of the cylinder opened and the pressures before and after the opening, the volume of the fuel rod can be calculated. To increase the precision of the results, four measurements are performed for each of the three cylinders with known volume. After every measurement the full system is completely evacuated.

Finally, by knowing the volume of the fuel rod and the pressure in the device when the gas was extracted, the pressure of the closed fuel rod can be calculated.

For every fuel rod three gas sample cylinders are filled with fission gas. For safety reasons gas sample cylinders are stored at pressures lower than atmospheric conditions, the filling pressures typically vary from 50 mbar up to 300 mbar. For this study a set of three gas sample cylinders for four different fuel rods was available for measurements.

Chapter 6

Mass spectrometry

6.1 Introduction

Mass spectrometry is an analytical technique for the determination of the elemental and isotopic composition of a sample.
Existing mass spectrometers differentiate for the physical principles used for the different processes from ion formation to ion detection. A summary of the main techniques used in modern MS devices is given in Figure 6.1.

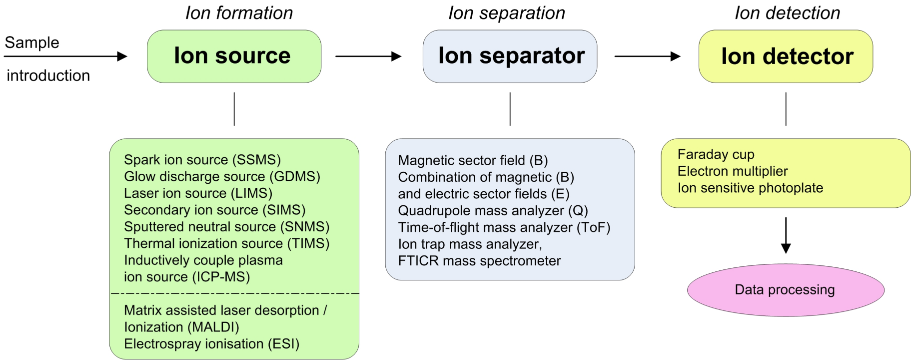

Figure 6.1: Basic diagram of mass spectrometry [22].

All types of mass spectrometers for analysis of inorganic and organic compounds are based on the same basic principles. The sample to be analyzed (gas, liquid or solid material) is inserted into the ion source. Liquids are introduced by nebulization of the solution and solids by evaporation, generally by laser ablation or electrothermal evaporation. In the ion source operating at high vacuum conditions, at low pressure or at atmospheric pressure, the sample material is vaporized, atomized and ionized, whereby mostly positively singly charged ions are used for analytical purposes. In the case of sector field MS the positively charged ions are extracted and accelerated from their original place of generation in the ion source to the entrance slit of the mass separation system (mass analyzer). Whereas the ion source normally is at a positive potential, the entrance slit has a potential of zero. After extraction of ions from the ion source to the entrance slit of the mass spectrometer, the ions have the potential energy qU_0, where U_0 is the acceleration voltage and q is the electrical charge of the considered ions (which can be expressed as Ze, where e represents the electric charge of the electron). The potential energy of the ions is completely transformed into kinetic energy after passing through the entrance slit. If the initial energy of the ions received upon formation is negligibly small in comparison to the accelerating energy of the ions by extraction to the entrance slit, the following equation is valid due the principle of the conservation of energy:

$$E_{kin} = qU_0 = \frac{1}{2}mv^2 \tag{6.1}$$

From this fundamental equation it can be concluded that the velocity of heavier ions is lower than the one of lighter ions and thus this difference can be directly used to determine the mass-to-charge ratio m/z.

6.2 Gas Source MS (GSMS) Balzers GAM 442

A gas source mass spectrometer is a special type of MS solely designed to work with gases. For general use GSMS is often combined with a gas chromatograph which gives additional information on the sample analyzed and eases the identification of unknown samples. However, when the constituents are known but not their concentration within the sample the importance of the gas chromatograph becomes marginal, and analysis can be done using only the mass spectrometer.

The general working principle of GSMS is the same as the one used by other types of MS. Ions are created in the ion source, are then separated according to their mass to charge ratio m/z and are finally detected by some type of detector. Thus, this section is focused on the differences between the MC-ICP-MS used for this study and the GSMS used as reference for fission gas analysis.

The Balzers GAM 442 is a GSMS with a quadrupole mass analyzer and an electron impact ionization source. A single Faraday cup or a secondary electron multiplier (SEM) are used as detectors. To introduce the gas in the mass spectrometer a system of high vacuum valves is applied. These valves are operated using a special computer controlled software.

Measurements of fission gas composition using Balzers GAM 442 are performed using a reference gas. This should have about the same composition as the fission gas concerning concentration of Xe, Kr, He and other components. However, natural elements are used for the fabrication of calibration gases and thus its isotopic composition differs from the one found in fission gases. GSMS applied to fission gas measurements can provide accurate results concerning concentration and isotopic composition. For concentration of Xe greater than 10% (n/n), relative uncertainties are usually below 1%. However, this rapidly grows when the amount of Xe is reduced, and below a concentration of about 1% (n/n) measurements become unreliable.

6.2.1 Electron Impact (EI) Ionization Source

If electrons of sufficient energy interact with the sample gas, positive ions are generated by the collisions. The electron beam is created inside the collision chamber in an EI source under vacuum conditions by using a heated filament (made of Rhenium in the case of the Balzers GAM 442). When a potential of 70 V is applied, the filament can reach temperatures of 1500–2000 K [23]. The sample is introduced perpendicularly respect to the electron current and the interaction between both species creates a cross beam of the ionized sample (Figure 6.2). The ions formed are then sent to the extraction lens perpendicular to the electron beam and finally driven to the mass spectrometer. Although EI ionization source has a poor ion yield, only small amounts of analyte are required for the ionization process.

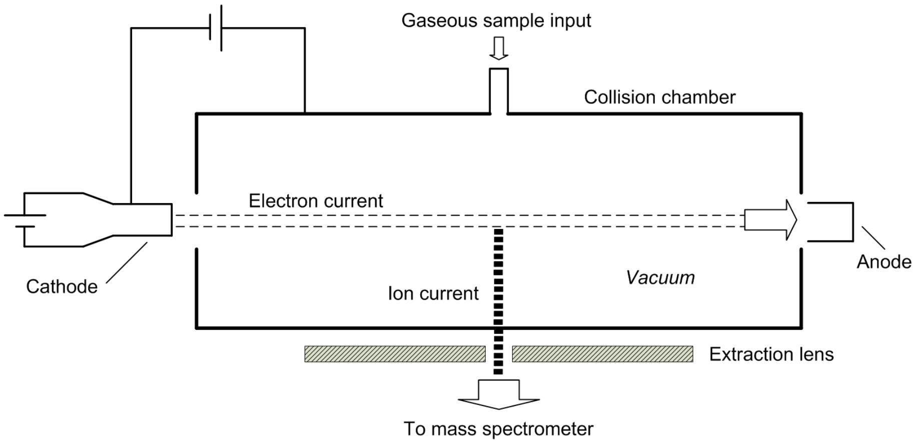

Figure 6.2: Electron Impact Ionization Source [22].

6.2.2 Quadrupole analyzer

The potential on the poles of the quadrupole is changed with a frequency ω. For a given frequency ω and voltage only ions with a mass between m and δm are able to pass the analyzer without colliding [24]. The ions having the selected mass collide in the detector generating an electric signal. By measuring the signal for different mass settings, the mass composition of the sample (and thus its isotopic composition) can be measured.

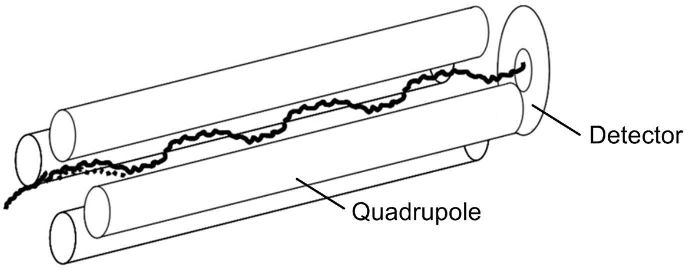

Figure 6.3: Quadrupole analyzer.

6.2.3 Advantages of GSMS

GSMS needs only a very small amount of analyte (for fission gases only 0.05 mLn) and allows to directly measure samples with high gas concentrations (from 10% (n/n) to 100% (n/n)) without any further dilution. The measuring process is completely automatized and the whole operation (from start-up of the machine until end of the measurement) requires only a couple of hours.

6.2.4 Disadvantages of GSMS

The detecting efficiency of the machine is very poor, many ions are lost between the source and the detector. This is a limit when measuring gases in small concentrations and contributes in increasing the relative uncertainty of the results obtained. Detection of different masses can only be performed sequentially, thus limiting the precision of isotopic ratio measurements.

6.3 Inductively Coupled Plasma Mass Spectrometry

Due to its excellent properties, inductively coupled plasma source (ICP) is currently the most commonly used ion source in inorganic mass spectrometry. Compared to established gaseous and solid state mass spectrometric techniques, the combination of an ICP ion source with a mass spectrometer is a relatively young analytical technique [22].

6.3.1 ICP ion source

The atmospheric pressure plasma in the ICP ion source is formed in a stream of an inert gas. A schematic of an ICP ion source including the quartz plasma torch and induction load coil together with sampler and skimmer as part of the interface region of an ICP mass spectrometer is shown in Figure 6.4. The ICP is sustained in a quartz torch consisting of three concentric tubes with different diameters. Ar, typically used in ICP-MS, flows through the concentric tubes of the ICP torch shown in Figure 6.4. The sample gas (or aerosol for liquid sample) is transported along the axis of the torch via the cooler, central channel tube at an Ar gas flow rate of 0.5–1.2 L/min. The auxiliary Ar gas flow is applied to push the plasma up above the top of the inner tube of the torch to prevent it from overheating.

For most applications only Ar of the highest purity is employed as plasma gas in ICP-MS. The Ar gas flowing between the outer tube and the intermediate tube (10–20 L/min) cools, in addition, the outer tube between the plasma and the load coil. An ICP source operates at RF frequency of 27 or 40 MHz and RF power of 1–2 kW. The high frequency field in the ICP is produced by the RF generator.

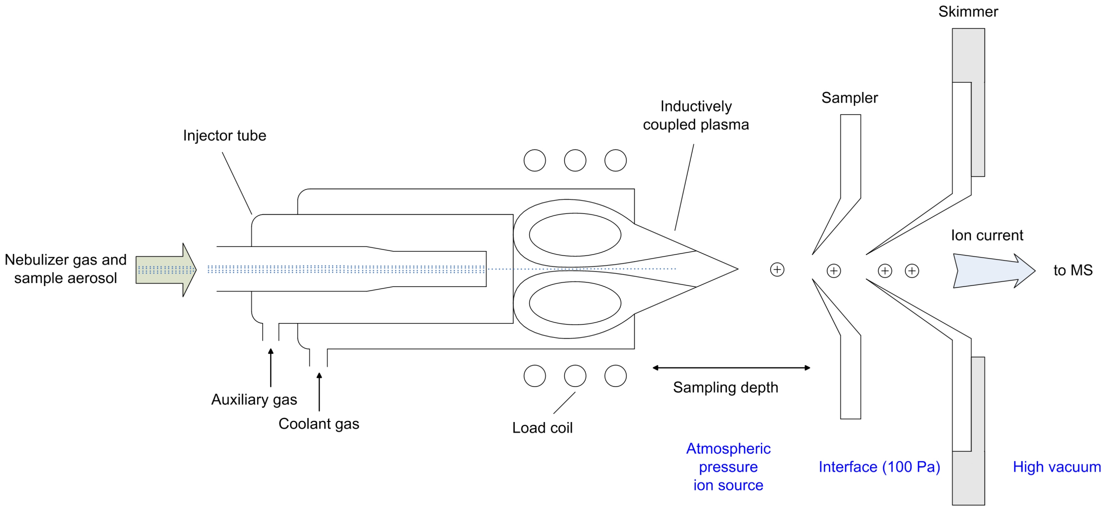

Figure 6.4: Schematic of an inductively coupled plasma source [22].

This energy input is transferred to the Ar gas at atmospheric pressure via the induction load coil. In order to ignite the Ar plasma discharge a tesla coil of high-voltage spark is employed and electrons are generated in the Ar gas. After the ignition of the plasma discharge, the electrons in the plasma are accelerated by the oscillating magnetic field and collide with atoms and molecules in order to ionize the plasma components. At a relatively high plasma temperature most of the sample gas is ionized into singly charged ions. The plasma temperature and electron number density are a function of the experimental parameters applied. Normally, ICP operates at a plasma gas temperature of approximately 5000–8000 K whereas the temperature of excited atoms is lower (between about 4000 and 6000 K). The electron temperature lies between 8000 and 10000 K, the electron density being about 1–3 $\cdot 10^{15}$ cm^{-3} [22].

The temperature of the ICP varies with the distance from the load coil and according to the setting of the ICP RF power and gas flow rate.

The ionization efficiency of an ICP source depends on the ionization energy E_i of the element to be analyzed. Elements with an ionization energy of less than 8 eV are ionized with nearly 100% yield [22]. With increasing first ionization energy, the ionization efficiency decreases. Having a first ionization potential of 12.13 eV, Xe has a poor ionization yield. At a plasma temperature of 7500 K the ICP ionization yield for Xe is between 3 and 4%.
To increase the ion transmission and to avoid secondary discharges, some mass spectrometer manufacturers (such as Thermo Fisher Scientific) employ a grounded conductive shield (e.g. of platinum or tantalum) which is located between the load coil and the ICP torch. Figure 6.5 presents a schematic of the shielded torch used by Thermo Fisher Scientific.

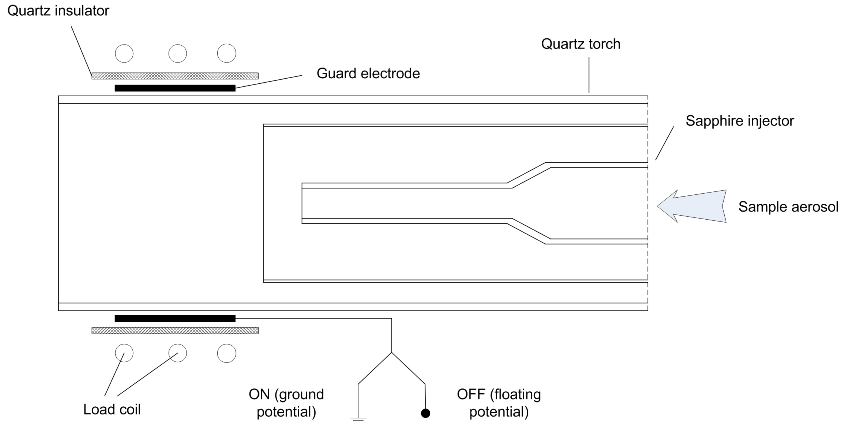

Figure 6.5: Schematic of shielded torch in ICP-MS [25].

6.3.2 Ion sampling interface

The sampling of the ions is performed through a series of chambers that are held at consecutively low pressures. The gas is sampled and transported from an area of high pressure to an area of lower pressure through a series of small orifices, as illustrated in Figure 6.4. By passing through the sampler orifice gas expands adiabatically, which causes a decrease in gas pressure and temperature creating an high speed directional flow able to transport ions in the vacuum. During the sampling step ions pass from the ambient pressure plasma of 7000 K into the mass spectrometer under high vacuum at room temperature. The gas flow speed increases and a supersonic jet is formed.
The pressure gradient is controlled in the interface, being the region between the sampler orifice and the skimmer cone. Most of the ions produced in the plasma pass the sampler cone, but about 99% [14] of them do not reach the skimmer cone and are removed from the system by rotary pumps.

6.3.3 Ion optics / focusing

Once the ions have passed the skimmer cone it is necessary to extract and focus them into the analyzer. Ion focusing is achieved by subjecting the charged ions to constant electric and magnetic fields. Electric fields are used to accelerate, shape and confine the ions, while magnetic fields are only employed to change the ions path using the Lorentz force ($\vec{F} = q(\vec{E} + \vec{v} \times \vec{B})$). Because photons are electrically neutral particles, the use of the magnets allows to avoid them reaching the detector, removing therefore sources of noise in the signal. Physically the ion optics is formed by an arrangement of quadrupoles (focusing magnets) and dipoles (bending magnets). This combination of magnets has the task of reducing the chromaticity and increasing the luminosity of the ion beam while keeping its flux constant.

6.3.4 Mass analyzer

The mass analyzer separates the ions extracted from the ICP source according to their mass to charge ratio (m/z) depending on the energy, momentum and velocity of the ions. A measurement of any two of these quantities allows the m/z to be determined. Successful operation of the mass analyzer requires a collision-free path for ions. To achieve this, the pressure in the analyzer section of the spectrometer should be as low as possible.
Different mass analyzers are used in ICP systems, the most frequently used being: quadrupole, double-focusing sector field and time of flight (TOF) mass analyzer.

6.3.5 Detector

Detectors are used to transform the ion current into an electric signal. In dynode detectors an incoming ion induces a cascade of electrons, amplifying therefore the ions signal. In Faraday cups incoming ions hit a metal or graphite cup and charge it. The current necessary to discharge it is measured. In addition to the Faraday cup, an amplifier is necessary to increase the signal strength.

6.3.6 Analytical performance

The isotopic information obtained by ICP-MS permits the use of isotopic dilution (see Chapter 3) for quantification, and the improved precision that accompany it. The detection efficiency for atomic ions is extremely high, in the case of Xe ion yield is about 50000 atoms per count. Moreover, those ions can be measured against an almost vanishingly low background, below 0.1 cps in the best spectrometers [16]. Due to its very high sensitivity ICP-MS only allows to measure elements in small concentration to avoid a saturation of the detectors. Therefore, several dilution steps are often necessary to prepare the sample to be analyzed.

6.3.7 Neptune MC-ICP-MS

This section focuses on the peculiarities of the MS used for this study, the Multi Collector ICP-MS "Neptune" (Thermo Fisher Scientific). In the following chapters its features and hardware are explained in more detail.

Features

The Neptune is a double focusing, high resolution multi collector mass spectrometer for high precision isotope ratio measurements. The instrument is composed of three modules illustrated in Figure 6.6: the ICP module, the Electrostatic Analyzer (ESA) module and the multi collector module.

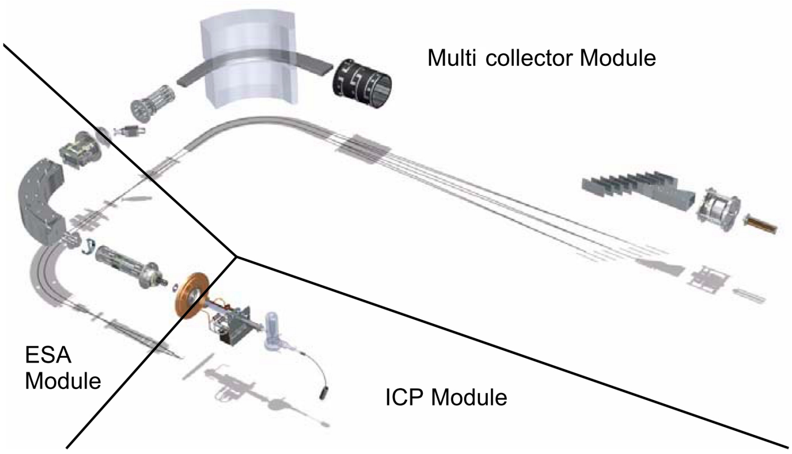

Figure 6.6: Components of the MC-ICP-MS "Neptune" [25].

ICP module

The ICP module (Figure 6.7) covers the hardware related to the plasma generation. It includes the mass flow controllers for the Ar supply, the RF generator, which powers the plasma and the XYZ stage to position the torch. Additional components of the module are the matchbox, which is responsible for the balance between the energy inside the plasma and the energy deliver to the load coil, the spray chamber and the torch itself.

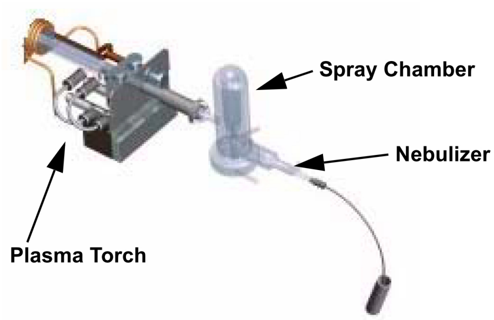

Figure 6.7: ICP module [25].

The sample is continuously fed into the nebulizer, where an Ar/sample aerosol is generated. The end of the plasma torch is located in the center of the load coil, which heats the gas with a radio frequency (RF) of 27.12 MHz. A spray chamber is used to remove the larger particles from the aerosol. Since only gas samples has been used in frame of this study, a simplified introduction system feeding the sample directly in the ICP was used. In the Neptune MS a guard electrode is used to improve the performance of the instrument and to avoid secondary discharges.

ESA module

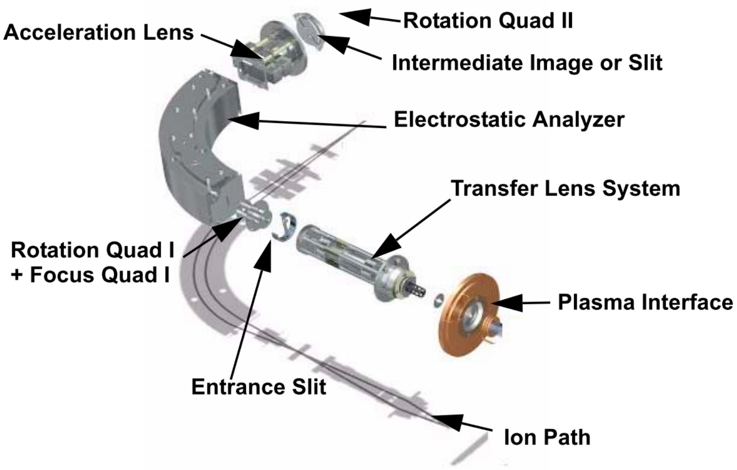

Figure 6.8: ESA module [25].

The ESA module (Figure 6.8) covers the hardware related to focusing and accelerating the ions. It includes the plasma interface, the transfer lens system, and the electrostatic analyzer (ESA).

The extraction lens is responsible for extracting the positive ions out of the main gas stream in the cone region and accelerate them to 2 keV kinetic ion energy. This lens is followed by a set of quadrupoles and ring electrodes to shape the ion beam and accelerate it further to 10 keV. Ions are then sent to the entrance slit which is used to set the instrument to one of the three resolution modes (low, medium or high). The electrostatic analyzer is mainly a spherical unit providing the electric field between two deflection plates. The electrical field bends and focuses the ions in respect to their energy. At the exit an intermediate slit is placed, used as an energy filter, which only allows ions with a narrow range of kinetic energy to pass it.

Multi collector module

The multi collector module (Figure 6.9) covers the magnet, the zoom optics, the multi collector, and the current amplifier system. The mass separation and the detection of ions take place in this module.

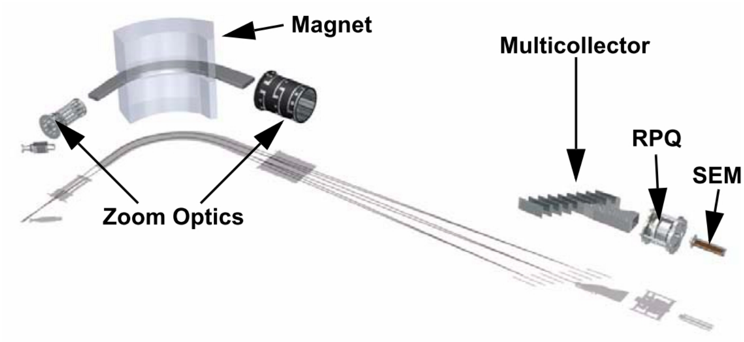

Figure 6.9: Multicollector module [25].

The magnetic sector separates and focuses the ions according to their mass to charge ratio to different positions along the focal plane (see Figure 6.10). The zoom optics can be used to change the spacing of the different masses along the focal plane (mass dispersion).

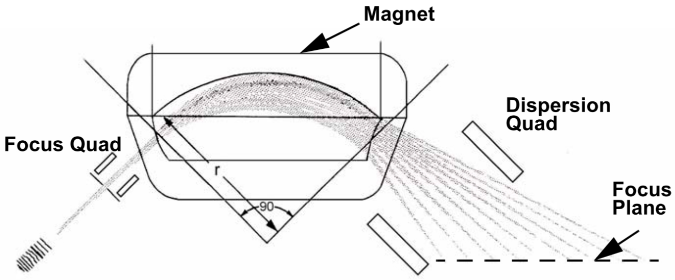

Figure 6.10: Schematic of the multicollector module [25].

The detectors are placed at the very end of the device. The multi collector is composed of nine identical Faraday cups. Eight of them can be moved by motor drives along the focal plane of the mass spectrometer to detect the different isotopes of most elements simultaneously. Each Faraday cup is connected to an amplifier which can increase the signal to a maximum of 50 V. The amplifiers are kept at constant temperature to avoid any temperature effect.

Chapter 7

Measuring methods with MC-ICP-MS

In this study gases with natural Xe isotopic composition have been used to perform test measurements in order to avoid wasting and releasing fission gas in the environment for testing purpose only. Natural calibration gases available on-site have been measured to check the capability of the mixing and diluting device (see Chapter 8). These gases have the same elemental constituents as fission gases, but their isotopic composition is natural. The composition of the two calibration gases used in this study is given in Table 7.1.

Table 7.1: Calibration gas composition.

Component	Gas 904		Bottle 13.950.6355	
	Concentration	Purity	Concentration	Purity
Xe	30.99% (n/n)	4.0	33.04% (n/n)	4.8
Kr	3.498% (n/n)	4.0	4.48% (n/n)	4.0
N_2	2.509% (n/n)	5.0	4.01% (n/n)	5.0
O_2	0.8406% (n/n)	5.0	0.500% (n/n)	5.0
CO_2	0.5165% (n/n)	4.5	0.999% (n/n)	4.5
Ar	1.014% (n/n)	5.0	1.491% (n/n)	5.0
He	Rest	5.0	Rest	4.6
Date of fabrication	03.04.2009		07.01.2006	
Guaranteed stability	24 months		24 months	

These gases are normally used for GSMS measurement in order to measure a calibration curve. The slightly different concentration of Xe between the bottles is used to simulate fission gases with different burnup (and thus different composition).

In this study, because of the use of MC-ICP-MS, calibration gases had to be diluted with Ar to a target concentration of about 20 ppm (n/n) to perform a measurement. Thus the results of measurements with MC-ICP-MS are in the ppm range, but using the dilution factor the original (undiluted) sample concentration can be calculated.

7.1 Measuring methods for natural Xe

Since the calibration gases have natural Xe composition, their concentration cannot be measured using IDMS. For this reason a different method has to be applied.
The output of MC-ICP-MS is an electric signal for every detector (corresponding to a specific isotope) which is measured in volt. This signal can be easily influenced by noise caused by small external changes in the environment. Thus normally ratios are used, which are more robust and have small uncertainties. For testing purpose absolute signal can be alternatively used to roughly estimate concentration of isotopes in the sample.
It is known that the signal intensity for a given isotope is proportional to its concentration. Thus, if the MS parameters are not changed for a given time, the time-averaged signal intensity can be used to estimate its concentration.
To keep the mass-flow rate of spike and sample constant over time two mass-flow controllers have been used. Their technical data are given in Table 7.2.

Table 7.2: Technical data of the mass-flow controllers.

Producer	Vögtlin
Model	red-y Smart Series
Range	0 - 25 mLn/min
Accuracy	± 0.3% F.S. and ± 0.5% of reading
Repeatability	± 0.1% of full scale
Operation pressure	0.4 - 11 bar

Two different modes have been used to estimate concentration of natural calibration gases: multi-injection mode and online mode.

7.1.1 Multi-injection mode

The sample gas is introduced in the MC-ICP-MS using an injector. When gas is injected in the device the signal increases rapidly, stays constant for a given time and then decreases when no more gas is available in the injector volume (for a detailed description of the injector's working principle see Chapter 8.3).

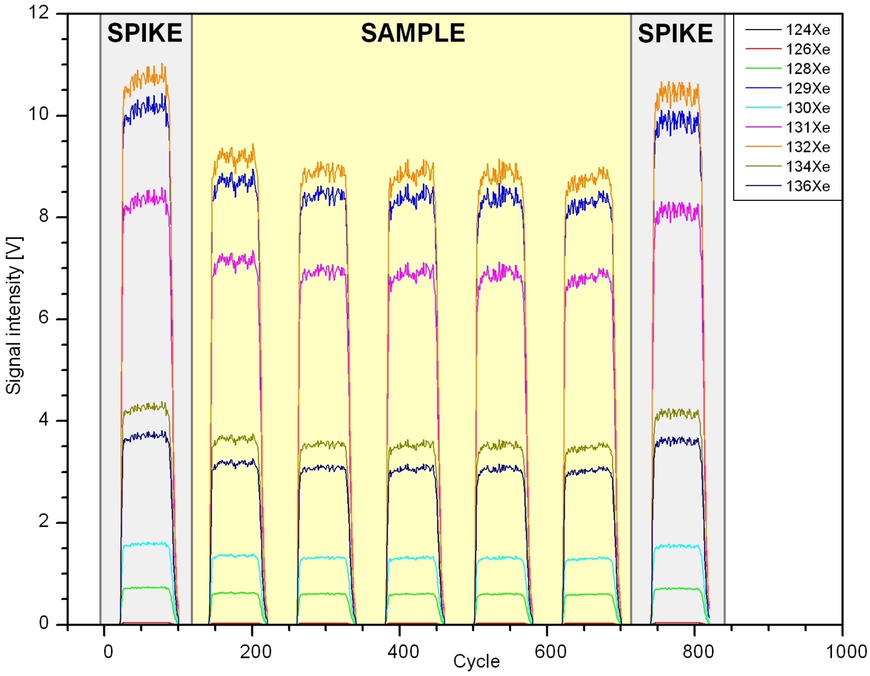

Figure 7.1: Multi-injection measurement.

In multi-injection mode the spike gas is initially introduced in the MC-ICP-MS. The response of the device is recorded and an average signal intensity is computed. Later, successive injections of the sample are performed and for each injection an average signal intensity is computed. At the end the spike is measured again to check the stability of the signal during the measurement sequence. It is known that the response of MC-ICP-MS changes from start-up of the machine because of internal changes. This phenomena is usually referred as instrumental drift. Measuring the spike at the beginning and end accounts for this effect and its influence on the results can be corrected (a typical measurement sequence using the multi-injection method is shown in Figure 7.1). In Figure 7.1 a cycle represents an integration of the signal from MC-ICP-MS over a user-given time (normally in the order of some seconds).

In multi-injection method spike and sample are introduced with the same mass-flow rate (usually 2 mLn/min).

7.1.2 Online mode

In online mode firstly the spike is introduced in the system at a constant mass-flow rate. When the signal has reached a sufficient stability the sample is injected in the system at the same constant mass-flow rate as the spike and the two species mix entering in the MC-ICP-MS. In this second step the signal increases again reaching a higher plateau. Analyzing the average signal intensity for both blend and spike the concentration can be easily estimated. The whole operation is then repeated many times to improve the statistics of the concentration data. A typical online measurement is shown in Figure 7.2.

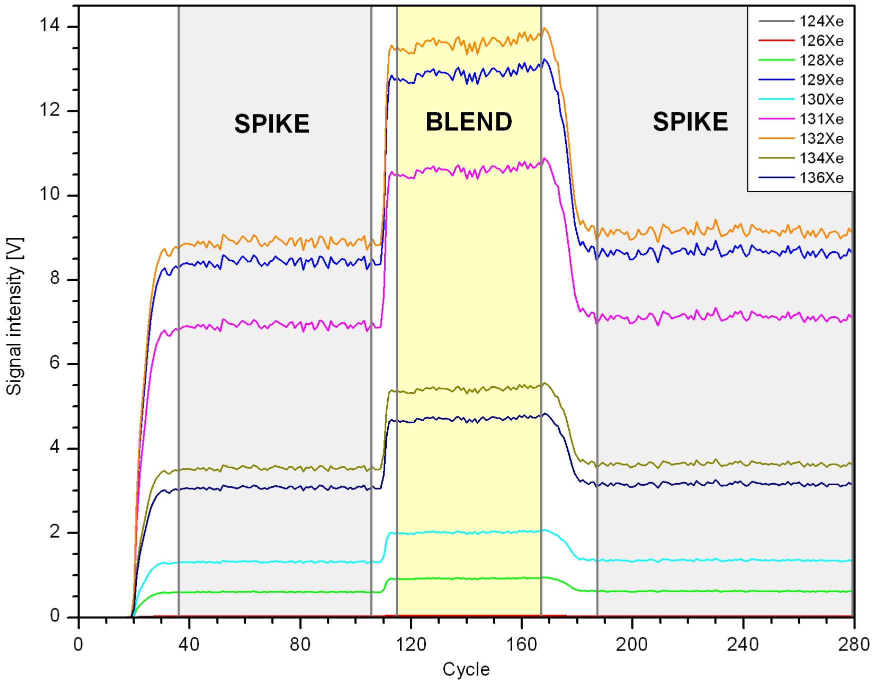

Figure 7.2: Online measurement.

Methods based on the signal intensity have the advantage of being easy to apply and therefore can be quickly used to estimate concentrations of natural Xe. This method can be applied to fission Xe as well, but because the precision of ratios is much higher than the one of the signal intensity, IDMS has been used when measuring fission gas.

A Microsoft Excel macro has been written to perform the calculation and the correction needed to compute the concentration starting from the absolute signal intensities given by MC-ICP-MS.

7.2 Measuring method for fission Xe

In case of Xe as fission gas the isotopic composition of spike and sample is different and thus IDMS can be applied. For this reason isotope ratios and not signal intensities represent the input data to compute the concentration. When applying IDMS only online measurements can be performed since the method is based on the difference in the isotope ratios between spike and blend. An example for a measurement with fission gas is shown in Figure 7.3. It is obvious that for isotopes not present in the sample the signal stays constant, while the ratio changes.

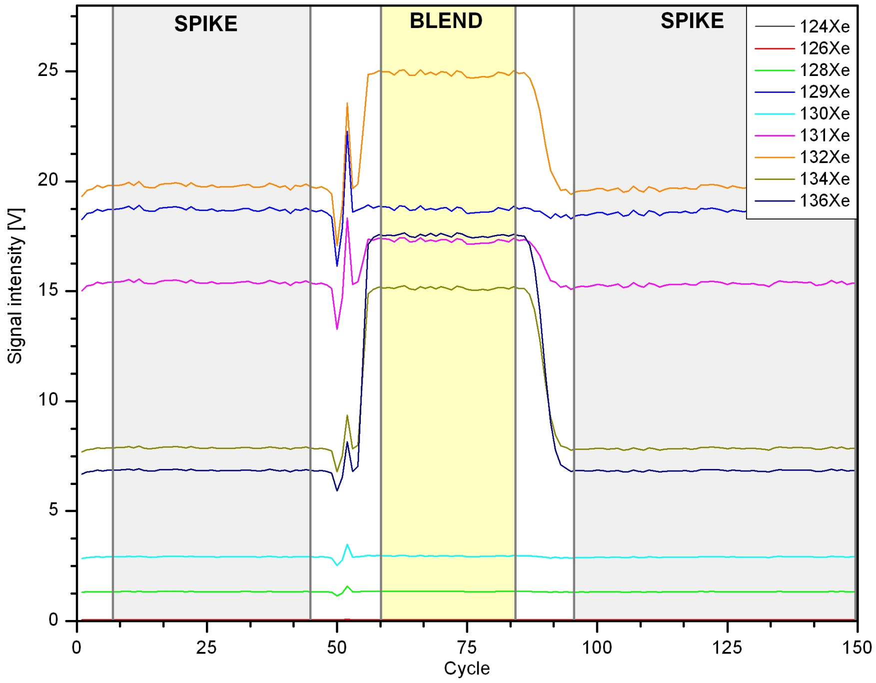

(a) Absolute signal intensity.

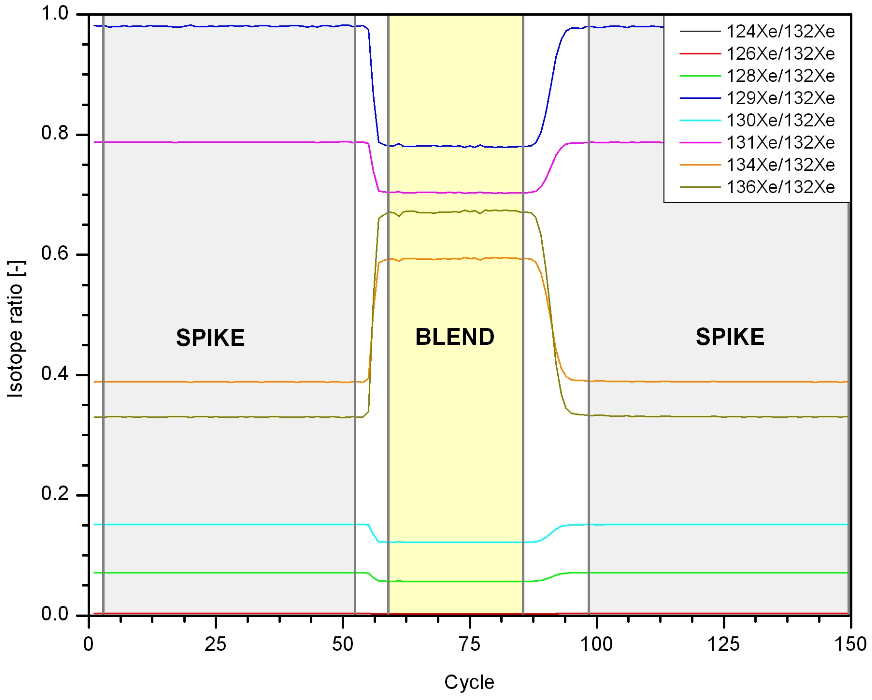

(b) Isotope ratio.

Figure 7.3: Fission gas measurement with MC-ICP-MS.

To compute the data obtained with ID-MC-ICP-MS a MATLAB program has been written (details are given in Appendix B). This automatically extracts the data from each measurement file, identifies the region of the blend and the spike and calculates the concentration of Xe within the sample. Additionally, uncertainty of the final result is estimated for a qualitative analysis.

Chapter 8

Mixing and Diluting Device (MDD)

8.1 Introduction

MC-ICP-MS is a very sensitive technique. A sample with a concentration of 100 ppm (n/n) Xe diluted in Ar can be enough to saturate the detectors. Typical fission gas samples have Xe concentrations in the order of 10% (n/n) to 50% (n/n) depending on the burnup. Direct measurement (like in the case of GSMS) are therefore impossible. Thus, in order to detect Xe by MC-ICP-MS a dilution is required.

Diluting liquid samples is a common practice in mass spectrometry and analytical chemistry. A wide range of laboratory equipment is available for this scope. In general, liquid mixtures homogenize very rapidly and a complete mixing can be achieved immediately. Thus very high dilution factors can be applied for liquid dilution and heterogeneity of the mixture is normally not a concern.

The situation is different for gas mixtures. An equilibration time in the order of weeks is often needed [26] if the diffusion process is not accelerated. Moreover, it is difficult to design gas mixing devices able to completely eliminate air contamination. In addition, the techniques related to gas mixing at low concentrations are not common in the field of mass spectrometry and the use of these techniques is often limited to very special applications far from the need of this study. Furthermore, existing devices can often only reach final concentration in the order of 1% (n/n) [27], not comparable to the target value of 20 ppm (n/n) required for fission gas measurement by ID-MC-ICP-MS.

Thus, designing a gas mixing and dilution device and improving its performance has been a central part of this study.

8.2 Gas mixing

8.2.1 Introduction

Because of the uncertainty of pressure measurements (especially close to vacuum conditions), gravimetric methods are often preferred instead of partial pressure methods for producing gas mixtures. The gravimetric method, despite its excellent capability in producing mixtures with a very accurate concentration (relative uncertainty ranges from 0.1 to 0.002% [27]), has the drawback of necessitating very expensive equipment to determine with sufficient precision the weight of gas bottles before and after the replenishment. For this reason, normally, only specialized industries can afford the costs related to this equipment and thus gravimetric mixtures are rarely prepared on-site in laboratories but usually delivered them by external providers.

Other methods, besides partial pressure and gravimetric methods, are available to produce gas mixtures, but for the specificity of this study cannot be employed. These are for example syringe injection and volumetric methods, which mostly apply to mixtures of fine dispersed liquid in gases.

8.2.2 Partial pressure method

If the partial pressure is precisely known, the amount of gases present in a defined volume can be measured. Since steel cylinders can work with different pressures, from vacuum condition to high pressures, high dilution factors can be easily achieved. With pressure or manometric techniques large volumes of complex gas mixtures can be generated and stored for future use. Several cylinders can be filled at the same time for relatively low cost. In addition, the dilution procedure can be repeated indefinite times with minimal changes in the equipment used.

Methods based on partial pressures with final concentration in the 180 to 380 ppm (n/n) range for small containers have been already used to prepare standard blends for mass spectrometric analysis ([28], [29] and [26]). Accuracies of ± 1% have been claimed for the dilution factor obtained in those gas samples. Different systems for producing gas mixtures based on manometric techniques with special properties have been patented already ([30], [31] and [32]).

A representative system to generate partial pressure mixtures is shown in Figure 8.1. The cylinders to be filled are connected to a manifold with an appropriate system of gauges over the pressure range of interest. The system should include a gauge in the vacuum region, since the manifold is usually evacuated to high vacuum before each component gas is introduced in the cylinder. The supply gases are normally connected to a separate manifold, and the two manifolds are connected with a valve.

A typical mixing procedure is performed in the following way. The system of manifolds and cylinders to be filled is evacuated and the first component flows into the empty cylinders. The desired pressure is reached and recorded. This must be done slowly to avoid errors from excessive temperature changes. All valves are closed and the manifold is again evacuated. The second component is introduced to the manifold at a pressure slightly in excess of the first component to prevent backflow of the filled component. The second component is then introduced to the test cylinder to the desired pressure. Additional components are introduced by repeating this same technique until all gases have been added. Low parts per million concentrations can be prepared by evacuating the system and introducing the trace contaminant through the system. The gas obtained can finally be measured using MS. The time required for mixing (mixture homogenization) must be considered. This time depends on the vessel size and geometry, injection turbulence, and the interdiffusion coefficients of the gases. If necessary the mixing of the gas components in the cylinders can be accelerated by rolling or heating.

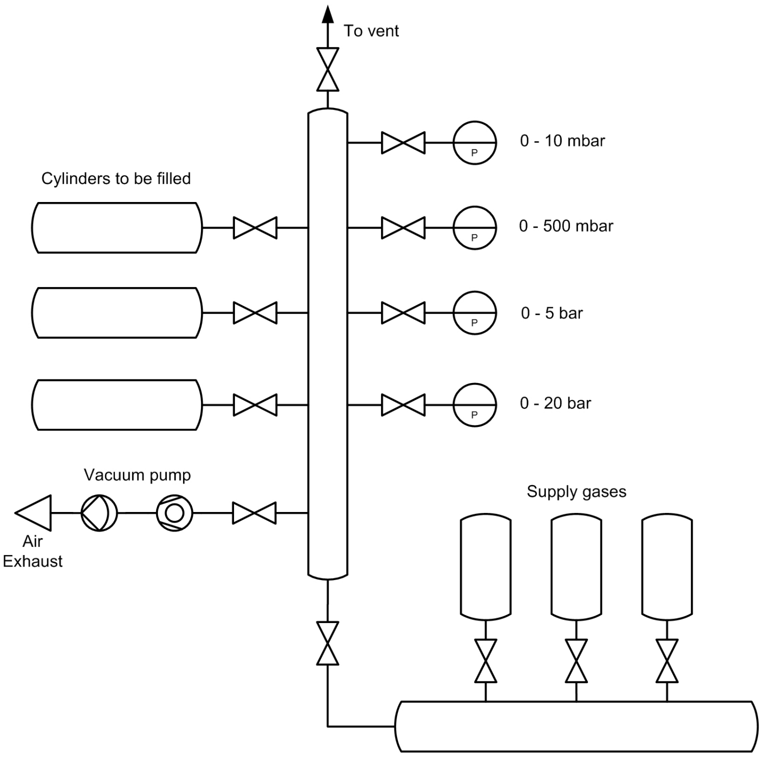

Figure 8.1: Sketch of a partial pressure system for filling gas cylinders [27].

Calculation of the gas mixture concentration can be performed assuming Dalton's law:

$$p_{\mathrm{tot}} = p_{\mathrm{a}} + p_{\mathrm{b}} + \ldots + p_n \tag{8.1}$$

where p_{tot} is the total pressure and $p_{\mathrm{a,b,\ldots},n}$ are the contributing partial pressures of the component gases. The concentration in parts per million by volume of each component at a given temperature is:

$$C_{\text{ppm (n/n)},n} = \frac{p_n}{p_{\text{tot}}} 10^6 \tag{8.2}$$

8.2.3 Ar compressibility

At room temperature and atmospheric pressure, most gases conform to the ideal gas law. However, at elevated pressures, deviations are pronounced and corrections of some percent are not unusual. This can be corrected by defining a new quantity, κ, the compressibility, which is given by:

$$\kappa = \frac{p_{\text{tot}} V}{RT} \tag{8.3}$$

where p_{tot}, V and T are measured experimentally to yield κ. Thus corrected, the concentration on the nth component can be expressed by:

$$C_{ppm(n/n)} = \frac{\frac{10^6 p_n}{\kappa_n}}{\frac{p_a}{\kappa_a^{'}} + \frac{p_b}{\kappa_b^{'}} + ... + \frac{p_n}{\kappa_n^{'}}} \tag{8.4}$$

where κ_n is the compressibility of the pure component at the filling pressure and $\kappa_{a,b,...,n}^{'}$ are the compressibilities of the gas mixtures at the final pressure.
Ar, as a noble gas, behaves similarly to ideal gases. However, compressibility effects cannot be completely neglected. Ar compressibilities at three temperatures are given in Table 8.1.

Table 8.1: Ar compressibility [33].

$T = 290$ K		$T = 295$ K		$T = 300$ K	
P [amt]	κ [-]	P [amt]	κ [-]	P [amt]	κ [-]
1	1.00000	1	1.00000	1	1.00000
2	0.99943	2	0.99957	2	0.99970
3	0.99875	3	0.99888	3	0.99901
5	0.99741	5	0.99766	5	0.99791
7	0.99589	7	0.99637	7	0.99685
10	0.99404	10	0.99455	10	0.99506
15	0.99068	15	0.99155	15	0.99242
20	0.98773	20	0.98876	20	0.98978
25	0.98437	25	0.98575	25	0.98713

Ar compressibility at 295 K (diluting temperature) and 6.5 bar (maximum Ar pressure reached during the diluting process) is 0.99680. This means that the bias caused by neglecting Ar compressibility in the concentration calculation is 0.3%. To avoid this all calculations for the concentration in this study have been performed considering the not-ideal behavior of Ar at high pressure.

8.2.4 Xe diffusion in Ar

As stated in Chapter 8.2.2 there are several factors influencing the homogenization time for gas mixtures. The interdiffusion coefficient of Xe in Ar is the only factor which can be modified without the need of changing the geometry or removing some parts of the device.

The diffusion process is related to geometry, time, temperature and pressure. In big volumes gas molecules/atoms can move for quite long distances before colliding with the wall and the distance they can freely travel does not depend on the direction of motion. On the contrary in small long pipes gas can only diffuse in the main pipe direction, since along the diameter the probability of colliding with the wall is very high. Thus, to increase the diffusion properties of gas systems, big volumes have to be used where the mixing is performed.

The influence of temperature and pressure can be easily estimated by using well known theoretical correlations for the diffusion coefficient. The most common method for the theoretical estimation of gaseous diffusion is the one developed independently by Chapman and by Enskog (1970). This theory leads to the equation [34]:

$$D = \frac{1.86 \cdot 10^{-3}\ T^{3/2}\ (1/\tilde{M}_1 + 1/\tilde{M}_2)^{1/2}}{p\sigma_{12}^2\Omega} \tag{8.5}$$

in which D is the diffusion (in $\frac{\mathrm{cm}^2}{\mathrm{s}}$), T is the absolute temperature (in K), p is the pressure (in atm) and the $\tilde{M}_i$ are the molecular weights.

σ_{12} and Ω are molecular properties characteristic of the detailed theory. The collision integral, σ_{12} (in Å), is the arithmetic average of the two species present. For Ar and Xe σ_{12} is given as (data from [35]):

$$\sigma_{12} = \frac{1}{2}(\sigma_1 + \sigma_2) = \frac{1}{2}(\sigma_{\mathrm{Ar}} + \sigma_{\mathrm{Xe}}) = \frac{1}{2}(3.543\text{Å} + 4.047\text{Å}) = 3.795\text{Å} \tag{8.6}$$

The collision integral Ω depends on an integration of the interaction between the two species. Its value can be found in tables as a function of the dimensionless number $\frac{\mathrm{k_B T}}{\epsilon_{12}}$, where ϵ_{12} represents the energy of interaction. For a binary system the energy of interaction is given by:

$$\epsilon_{12} = \sqrt{\epsilon_1 \epsilon_2} \tag{8.7}$$

Thus the dimensionless quantity $\frac{\mathrm{k_B T}}{\epsilon_{12}}$ in the case of Ar and Xe at room temperature (293.15 K) is (data from [35]):

$$\frac{\mathrm{k_B}T}{\epsilon_{12}} = \frac{\mathrm{k_B}T}{\sqrt{\epsilon_1\epsilon_2}} = \frac{\mathrm{k_B}T}{\sqrt{\epsilon_{\mathrm{Ar}}\epsilon_{\mathrm{Xe}}}} = \frac{1.3807 \cdot 10^{-23}\frac{\mathrm{m^2kg}}{\mathrm{s^2K}} \cdot 293.15\mathrm{K}}{\sqrt{1.2882 \cdot 10^{-21}\mathrm{J} \cdot 3.1893 \cdot 10^{-21}\mathrm{J}}} = 1.9968 \tag{8.8}$$

The collision integral Ω can now be calculated using the tabulated value from Hirschfelder [35].

$$\Omega = 1.0756 \tag{8.9}$$

Therefore, the interdiffusion coefficient of Xe in Ar at atmospheric pressure is calculated using Equation 8.5 as:

$$D = \frac{1.86 \cdot 10^{-3} \cdot 293.15^{3/2} \cdot (1/39.948 + 1/131.293)^{1/2}}{1 \cdot 3.795^2 \cdot 1.0756} = 0.1089\ [\frac{\mathrm{cm}^2}{\mathrm{s}}] \tag{8.10}$$

The experimental value at atmospheric pressure and 329.9 K temperature is 0.137 $\frac{\mathrm{cm}^2}{\mathrm{s}}$ [34]. Using the procedure described above for the same temperature one obtains 0.135 $\frac{\mathrm{cm}^2}{\mathrm{s}}$. Thus, the Chapman and Enskog theory can describe with good accuracy the phenomena of diffusion of Xe in Ar.

It is important to note that the diffusion coefficient is depending on both temperature and pressure. This double dependence has to be considered when heating a gas container. There is not only the temperature increased but the pressure increases too. An adaptation of Equation 8.5 for heated systems with constant volume can be done by applying the ideal gas law. Considering the compressibility, the pressure inside a closed volume can be described by:

$$p = \frac{\kappa n \mathrm{R} T}{V} \tag{8.11}$$

where n is the amount of gas, R the gas constant, V the volume and κ the compressibility. This equivalence can be inserted in Equation 8.5 to obtain a dependence on temperature only.

Figure 8.2 illustrates the diffusion coefficient in function of the temperature for the geometry and the condition used in this study (main volume about 0.5 L, heating started at about 6.5 bar and 296 K).

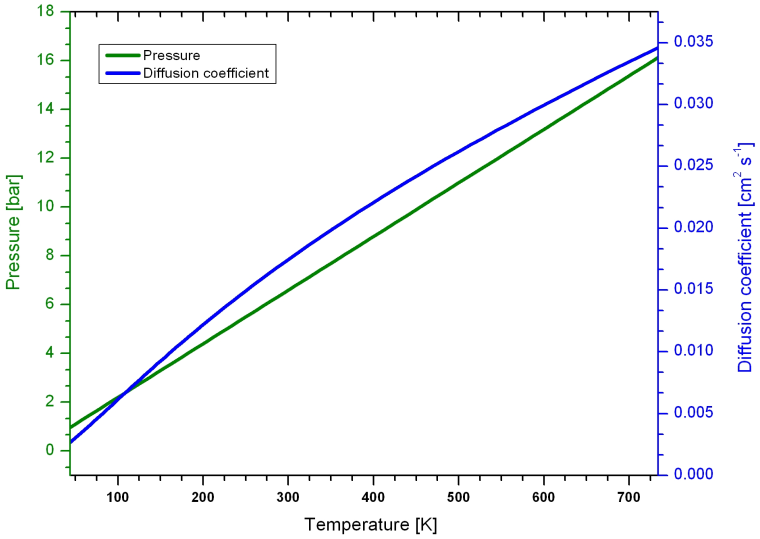

Figure 8.2: Diffusion coefficient in a closed volume.

It can be noticed that although the increasing pressure has a negative effect, the diffusion coefficient is almost doubled when a temperature of about 700 K is reached.

The diffusion process has a time-dependence described by exponential laws. This means that even an increase of the diffusion for a short time (by heating at high temperatures) can have big benefits on the internal mixing process of the gas sample.

8.3 MDD prototype

The mixing and diluting device (MDD) is the tool which has been build for the scope of this study, i.e. dilute fission gas in order to measure the concentration of Xe with MC-ICP-MS. The working principle of this device is very similar to the one described in Chapter 8.2.2. Partial pressure measurements are used to determine the quantity of gases introduced.
The device is composed of a series of cylinders with a defined volume (10 – 500 mL) connected by a common pipe. This pipe is linked to the vacuum pump, which allows to evacuate the system before and after every dilution step. A schematic of the prototype version of the MDD (designated and manufactured before the start of this study) is given in Figure 8.3, while in Table 8.2 its main components and their technical date are listed.

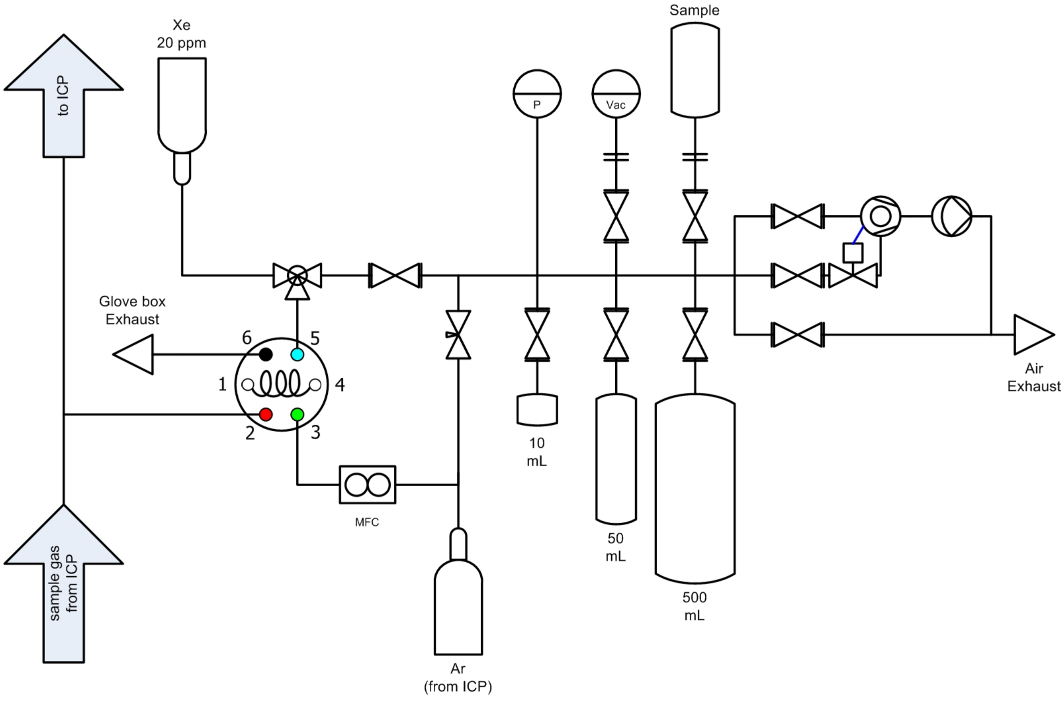

Figure 8.3: Mixing and diluting device prototype

At the exit of the device a mass-flow controller has been applied to check or measure the mass-flow rate of gas to the MC-ICP-MS during the measurement. An injector with a volume of about 3.5 mL has been used to inject rapidly the diluted sample gas into the main Ar flow transporting it directly to the MC-ICP-MS. This injector is connected to both the Ar flow going to MC-ICP-MS and the mixing and diluting device (a schematic of the injector is shown in Figure 8.4). When the injector is set on load position the diluted gas fills the injector loop and is finally dispersed in the exhaust. In the load position the mass spectrometer is constantly flushed with Ar. When the injector is switched to the inject position the Ar flow transports the diluted sample gas from the loop to the MC-ICP-MS. In this position the sample gas coming from the MDD bypass the loop and goes directly to the exhaust.

Table 8.2: Technical data of the main components of the MDD.

	Vacuum gauge	Pressure sensor
Manufacturer	Pfeiffer Vacuum	Keller Druck
Model	CMR 362	LEX1
Range	0.01 - 110 mbar	0 - 21 bar
Accuracy	0.2% of reading	0.05% F.S.
Precision	N.D.	0.05%
Resolution	0.003% F.S.	1 mbar

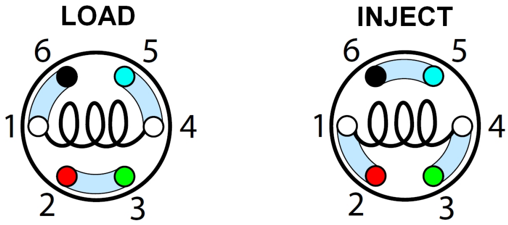

Figure 8.4: Schematic of the injector; connections 2 and 3 are connected to the carrier or the spike (depending on the configuration), connections 5 and 6 to the sample.

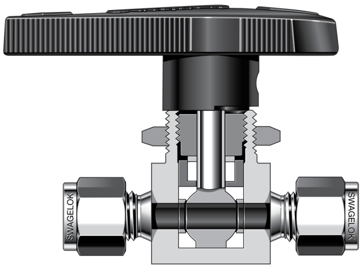

Figure 8.5: Schematic of the ball valves (Swagelok).

The 40 Series ball valves of Swagelok have been used in all valve positions. A schematic of this type of valve is given in Figure 8.5. Although not being specifically designed to work under vacuum conditions, this type of valve has been chosen

because of its capability to work with high pressures (up to 172 bar).
Figure 8.6 shows the MDD prototype including the turbomolecular pump used to evacuate the system and the mass-flow controllers. The cylinders and the connections between them are fixed below the metal plate and the valves are commuted from above the plate.

Figure 8.6: Mixing and diluting device prototype.

Part III

Results and uncertainty consideration

Chapter 9

Results and discussion

9.1 MDD version 1.0 (prototype)

9.1.1 Dilution procedure

Dilutions using the MDD version 1.0 (prototype) have been performed in two dilution steps. Firstly the system has been completely evacuated. Then the 10 mL volume has been filled with sample gas to a pressure of about 5 mbar. This pressure has been recorded with the vacuum gauge. The valves separating the 50 and 500 mL cylinders have been closed before the insertion of gas and thus were left under vacuum condition. Once the pressure has been accurately recorded the system is filled with 0.5 bar Ar to perform the first dilution step. The pressure is now recorded using the pressure sensor. At this moment the valves of the 50 and 500 mL cylinders are opened. Since these were left under vacuum the pressure in the complete system decreases, reaching a value of about 40 mbar, recorded by the vacuum gauge. Finally, the system with all cylinders is filled with Ar at 6.5 bar. These two dilution steps result in an overall dilution factor of about 16000.
With this procedure fission gas with a Xe-content of 30% (n/n) can be diluted to less than 20 ppm (n/n).

9.1.2 Natural Xe measurements

The gas contained in the bottle 13.950.6355 (see Table 7.1) has been diluted using MDD version 1.0 from an initial Xe concentration of 33.04% (n/n) to a target concentration of 20 ppm (n/n). The diluted gas has then been measured using the multi-injection mode explained in Chapter 7.1.1. When the injector is in load position the pressure in the system gradually decreases from the initial value of 6.5 bar, reached at the end of the dilution, to atmospheric pressure. The results for a sequence of three independent injections with different homogenization time are shown in Table 9.1.

Table 9.1: Xe concentration (n/n) of gas diluted using MDD version 1.0.

Homogenization time	20 min	100 min	1000 min
First injection	6.22 ppm	18.90 ppm	17.68 ppm
Second injection	22.15 ppm	19.72 ppm	17.72 ppm
Third injection	29.58 ppm	20.21 ppm	17.82 ppm
Average	19.32 ppm	19.61 ppm	17.74 ppm
Relative STD [1] ($1s$)	61.77%	3.36%	0.39%
Trend	Increasing	Increasing	Increasing

Analyzing the results it can be observed that the homogenization time has a dramatic influence on the results. The measurement performed 20 minutes after the dilution shows an evident trend. The same trend can be observed in the measurements performed after longer homogenization time (100 and 1000 minutes), although to a much lesser extent.

Looking in more detail at the design of the device it can be noticed that all the cylinders used for the dilution have single-sided connections. The use of these cylinders has been assumed as the major cause for the big trend observed in the first measurements. During the first dilution step the sample gas distributes uniformly in all the cylinders opened. When Ar is introduced to dilute the sample, this gas pushes the sample to the closed end of the cylinder resulting in a stratification of both gases. Diffusion enables the homogenization of gases in the system but even after 1000 minutes a good mixture quality cannot be achieved and some stratification is still observable. Complete homogenization can be expected only after very long time because big volumes are connected by small pipes where diffusion is retarded.

For all measurements with the MDD version 1.0 the average concentration value for Xe was determined to be less than the target value (20 ppm (n/n)).

9.2 MDD version 1.1

9.2.1 Concept

A schematic of the adopted device (version 1.1) is shown in Figure 9.1. The main improvement of this version is the connection of the main cylinder (500 mL) on both sides and a reduced number of dead volumes in the parts used for the dilution. The

---

[1] Standard Deviation

10 and 50 mL volumes have been completely eliminated from the design and the connection between the two valves preceding the main cylinder (indicated in blue in Figure 9.1) have been used as intermediate volume for the dilution procedure. This intermediate volume and the total volume between the valves connecting the main cylinder have been accurately measured gravimetrically by filling them with pure water and measuring the change in mass with and without water. The ratio between both volumes has been determined as 65.69.

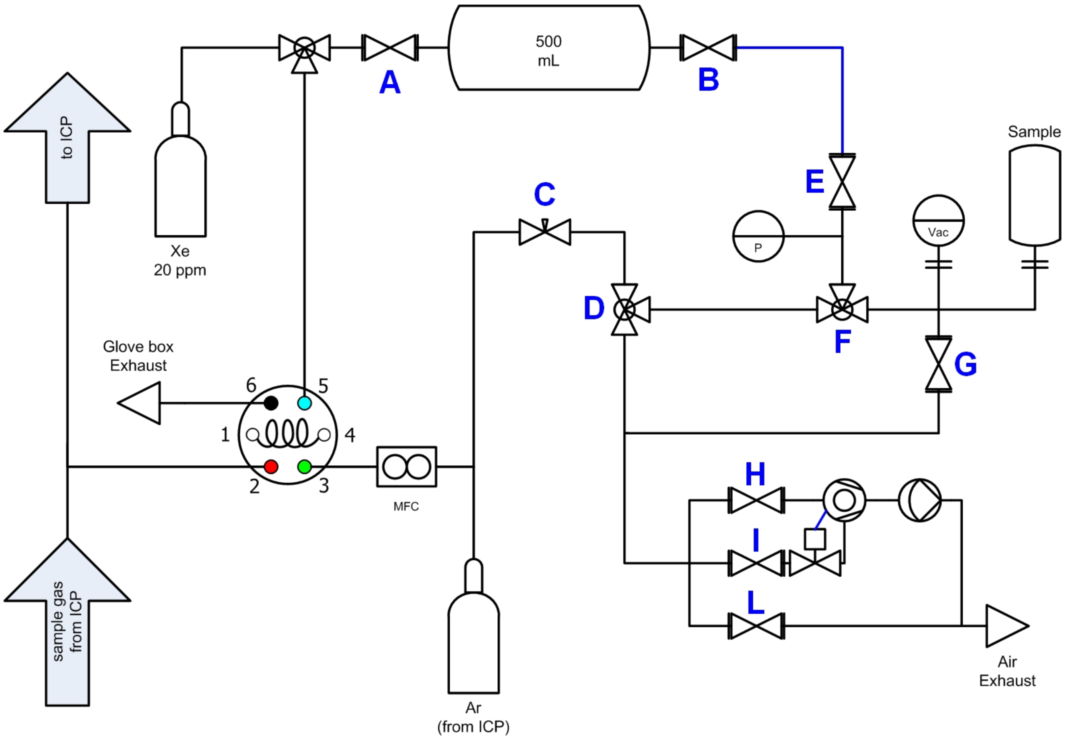

Figure 9.1: Mixing and diluting device, version 1.1.

9.2.2 Dilution procedure

Dilution experiments with the MDD version 1.1 have been performed as follows. All the internal valves (B, E, F, G and H) of the device have been opened and the system was evacuated. The valves on the main cylinder (A and B) have been closed and the sample gas has been filled in the rest of the system at a pressure of about 25 mbar. The valves on the intermediate volume (B and E) have been closed and then the one between the intermediate volume and the main cylinder (B) has been opened and the gas has uniformly distributed in both spaces. Since the ratio between both volumes is precisely known the pressure reached by this expansion can be easily computed. A pressure of about 0.4 mbar is reached in this second step. Afterwards, pure Ar is introduced in the system at a pressure of 6.5 bar to perform the final dilution step. Dilution factors of more than 16000 can be reached.

9.2.3 Natural Xe measurements

A typical result for a measurement of calibration gas (bottle 13.950.6355) diluted to a target concentration of 20 ppm (n/n) using MDD version 1.1 is given in Table 9.2.

Table 9.2: Xe concentration of gas diluted using MDD version 1.1.

Homogenization time	20 min
First injection	20.54 ppm (n/n)
Second injection	18.70 ppm (n/n)
Third injection	18.70 ppm (n/n)
Average	19.31 ppm (n/n)
Relative STD (1s)	5.51%
Trend	Decreasing

It can be observed that the concentration is much higher in the first injection than in the following ones. This suggests that the mixing is still very heterogeneous.
In fact although the main cylinder has now been connected on both sides, the Ar and the sample always enter on the same side (right in Figure 9.1) during the dilution process. The left side of the cylinder is only used to extract the gas to perform the MC-ICP-MS measurements. Again stratification of sample gas in the main cylinder can explain the results of the measurement. Sample gas is pushed to the left side when the dilution is performed and therefore the high concentration is measured in the first injection.
As for the prototype (version 1.0) it has been observed for version 1.1 that the measured concentration is always below the target value.
Summarizing with MDD version 1.1 the quality of the results concerning the reproducibility at a short homogenization time has been improved, but stratification and heterogeneous mixing are still a concern which need to be eliminated.

9.3 MDD version 1.2

9.3.1 Concept

To solve the problems of stratification of gas and mixture heterogeneity encountered, a revised version has been designed by changing the geometry of the system.

A schematic of the design for this version 1.2 is shown in Figure 9.2. The main improvement of the new design is to use both sides of the main cylinder to dilute the sample gas. If Ar enters on both sides of the main cylinder, counter currents are formed internally, which generate turbulences that can greatly increase the mixing capability. Thus introducing Ar at the same time on both sides should avoid stratification effects. Additionally, in the MDD version 1.2, a plate heater has been placed under the main cylinder to enhance the diffusion of the gas mixture.

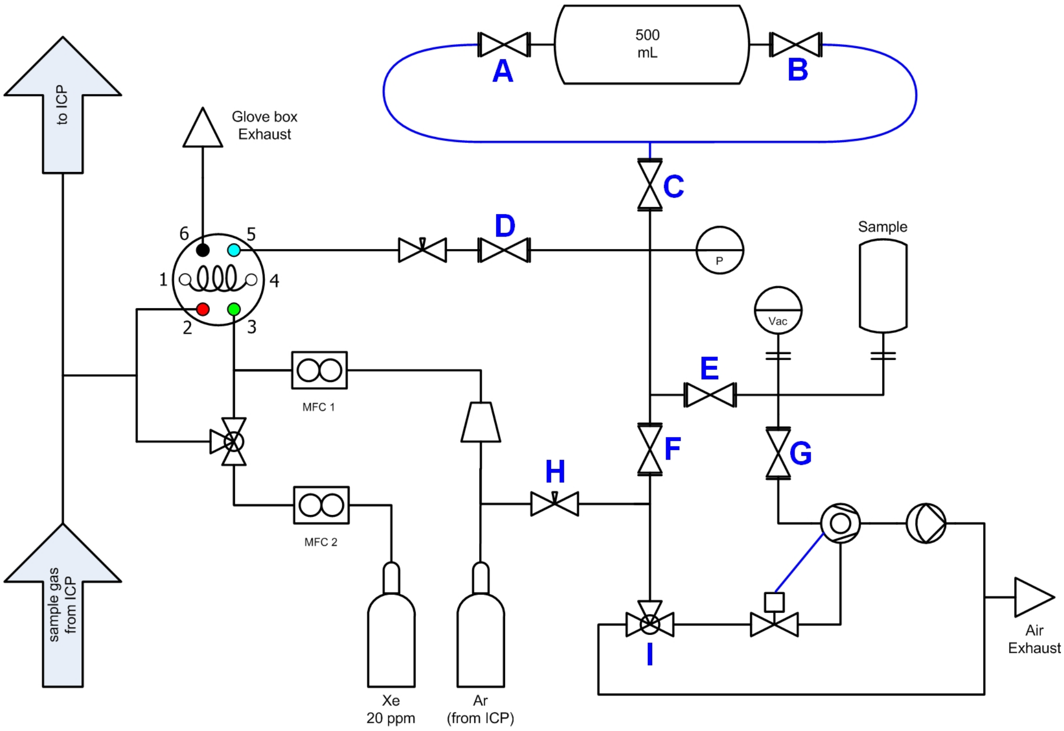

Figure 9.2: Mixing and diluting device, version 1.2.

Heating was applied for two reasons:

1. By increasing the temperature of the gas in the main cylinder, the interdiffusion coefficient of Xe in Ar increases too (see 8.2.4). This has a considerable effect on the capability of internal homogenization of the mixture.
2. A non-uniform heating has been deliberately created by placing the heater at the bottom and leaving the upper surface at free contact with air. This setup produces temperature differences between upper side and lower side

> of the wall, that drive circular internal flows. At a bottom temperature of about 300°C, the difference between cold and hot side has been measured as about 150°C. This difference is sufficient to generate internal turbulences improving the gas mixing within the cylinder.

A standard plate heater of 700 W maximum power able to reach 400°C has been used in the MDD version 1.2. To cool quickly the gas to ambient temperature before starting the measurements a water bag has been placed on the cylinder.

Again, the pipe volume preceding the 500 mL cylinder (indicated in blue in Figure 9.2) has been used as intermediate volume for the dilution. The volume ratio has been measured gravimetrically by filling the volumes with pure water and measuring the weight difference with and without water. The volume ratio has been determined as 32.54.

Special attention in the design has been paid in minimizing the volume of sample needed to perform a dilution. This 35 mL minimal volume has been determined. Therefore, samples with a pressure of 22 mbar and a volume of 50 mL (standard volume for fission gas samples) can be successfully measured. Samples with lower pressures can be measured too, but a higher uncertainty in the results has to be taken into account.

9.3.2 Dilution procedure

Dilution experiments with the MDD version 1.2 have been performed in two ways: directly or indirectly. For both cases all the external valves (D, H and I) have been closed firstly and the internal volume has been evacuated till a sufficient vacuum has been reached (usually less than 0.001 mbar). For the direct mode the main cylinder has then been filled directly with sample gas at a pressure of about 0.4 mbar and then diluted with 6.5 bar Ar by opening simultaneously both valves at the extremities (A and B). In the indirect mode the valves on the main cylinder (A and B) have been closed and the intermediate volume has been filled with 13 mbar of sample gas. The intermediate volume has then been insulated and the valves on the main cylinders (A and B) were opened. The pressure in the cylinder after depressurization can be calculated knowing the volume ratio. This is usually about 0.4 mbar. Finally, the main volume has been filled with Ar at maximum pressure (6.5 bar) by opening at the same time the valves on both sides (A and B). For the direct and the indirect mode dilution factors of more than 16000 can be achieved.

When the dilution is finished the plate heater is turned on to improve the mixing kinetic. Temperatures of 300°C at the bottom were reached and maintained for several hours. At this temperature the interdiffusion coefficient of Xe in Ar is nearly doubled compared to ambient temperature.

9.3.3 Natural Xe measurements

Typical results for a multi-injection measurement of a calibration gas sample (bottle 13.950.6355) diluted from a Xe-concentration of 33.04% (n/n) to a target of 20 ppm (n/n) are shown in Table 9.3.

Table 9.3: Xe concentration of gas diluted using MDD version 1.2.

Homogenization time	5 min	120 min
Heating	OFF	ON
1st injection	22.51 ppm (n/n)	21.03 ppm (n/n)
2nd injection	21.44 ppm (n/n)	20.93 ppm (n/n)
3rd injection	21.01 ppm (n/n)	21.09 ppm (n/n)
4th injection	20.74 ppm (n/n)	20.99 ppm (n/n)
5th injection	20.39 ppm (n/n)	21.03 ppm (n/n)
6th injection	20.31 ppm (n/n)	20.94 ppm (n/n)
Average	21.07 ppm (n/n)	21.00 ppm (n/n)
Relative STD ($1s$)	3.88%	0.29%
Trend	Decreasing	None

It can be observed that the mixture homogeneity after only 5 minutes of homogenization time is much better than the one observed after 20 minutes with the previous versions of the MDD. A weak trend can still be observed from the first to the last injection after five minutes of homogenization. This trend completely disappears when the heater is used to improve the mixing process. The mixture obtained by heating the gas finally shows a satisfying concentration distribution and thus an almost complete mixing can be assumed when using MDD version 1.2 in combination with the heater.

For both cases (with and without the use of a heater) it can be noticed that the concentrations measured are slightly larger than the target value of 20 ppm (n/n). This observation is in contrast with the results obtained with the previous versions, where the concentrations obtained were below the target value.

9.3.4 Fission Xe measurements

Using MDD version 1.2 fission gases from a Swiss NPP have been measured additionally to inactive gas measurements reported above. The results obtained with MC-ICP-MS have been compared with the ones of GSMS. The data are shown in Table 9.4.

Table 9.4: Xe concentration of fission gases measured with GSMS and MC-ICP-MS diluted using MDD version 1.2.

MC-ICP-MS			
Fission gas sample	FBA004-B3	FBA004-B3	FBA004-B3
Homogenization time	300 min	280 min	390 min
Heating	ON	ON	ON
1st injection	7.77% (n/n)	8.58% (n/n)	10.77% (n/n)
2nd injection	7.78% (n/n)	8.59% (n/n)	10.71% (n/n)
3rd injection	7.73% (n/n)	8.44% (n/n)	10.72% (n/n)
4th injection	7.73% (n/n)	8.44% (n/n)	10.67% (n/n)
5th injection	7.75% (n/n)	8.36% (n/n)	10.71% (n/n)
6th injection	7.73% (n/n)	8.42% (n/n)	10.74% (n/n)
7th injection	7.73% (n/n)	8.55% (n/n)	10.74% (n/n)
8th injection	7.74% (n/n)	8.51% (n/n)	10.74% (n/n)
Average	7.74% (n/n)	8.49% (n/n)	10.73% (n/n)
Relative STD (1s)	0.27%	0.97%	0.28%
Trend	None	None	None
GSMS			
Average concentration	14.77% (n/n)	14.89% (n/n)	14.85% (n/n)
Relative uncertainty (1s)	0.19%	0.13%	0.19%

The overall precision of the results is better than 1%. Thus MDD version 1.2 combined with heating is a valuable instrument to achieve homogeneous mixtures. However, the absolute concentrations obtained are not consistent with the data obtained using GSMS. Possible explanations will be discussed in the following sections.

9.4 Conclusions on MDD version 1

MDD has improved its mixing capability from version 1.0 to version 1.2. The relative standard deviation between different injections has been reduced from more than 50% to less than 1%, achieving in some cases, when IDMS is applied, values even better than 0.3%. In addition to this the homogenization time needed to reach good mixture quality (less than 1% of relative standard deviation) has been reduced from more than 10 hours to less than two hours. Combining all the measurements obtained with inactive gas using MDD version 1.2 it can be seen that homogeneous mixtures can be reached in a couple of hours (see Figure 9.3).

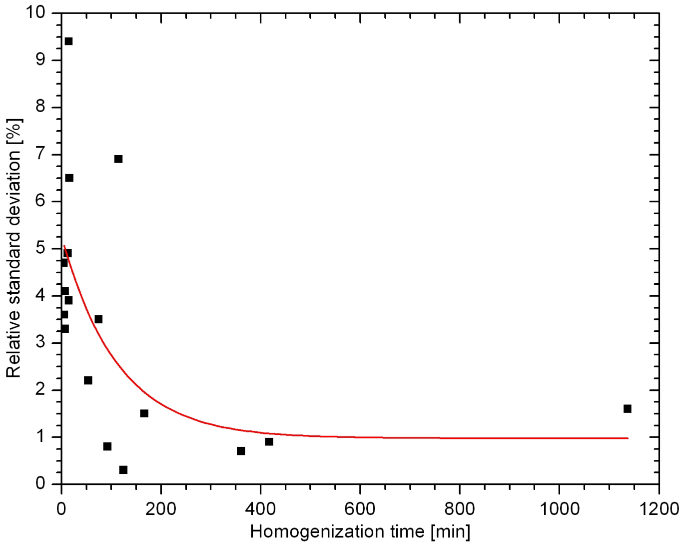

Figure 9.3: Relative standard deviation of the Xe concentration obtained for different injection with MDD version 1.2.

However, although improvements have been made concerning mixture homogeneity, the absolute concentration obtained always are significant different from the expected value. For MDD version 1.0 and 1.1 the concentration measured was below the one expected for inactive gas, while in MDD version 1.2 this was higher than expected for inactive gas and much lower for fission gases.

9.4.1 Leak rate

For systems working under vacuum conditions the leak rate is the rate for which the external gas (typically air) penetrates inside the system. This is normally measured in mbar L^{-1} s^{-1} and can be estimated by insulating the system and measuring the internal increase of pressure or using special devices which often allow local leak rate detection.

The leak rate of the whole system of pipes and volumes of the MDD (version 1.0 to 1.2) was about 0.0003 mbar L^{-1} s^{-1}. This value has decreased over the time since solid particles in the air tend to close small leaks in the connection between different parts. In the MDD the leak rate was unequally distributed in the system, and especially close to the main cylinder the local leak rate has been found being higher than in other components.

Due to the type of valves used in the design it has been difficult to completely evacuate the system. In fact the small ball contained in the valves (see Figure 8.5) represents a dead volume when the valve is closed. This does not allow a complete evacuation for the valves that have to remain closed during the evacuation procedure.

It must be considered that air contamination occurred during the dilution when the pressure had to be reduced below atmospheric pressure. Since air contains a very low concentration of Xe, it has to be considered as a dilutant, like pure Ar normally used. Thus, because of the contribution of air, lower concentration than the one expected should be measured when gas is diluted using a device which is not sufficiently insulated again external contamination. Consequently a dilution lasting long time should be more effected by air contamination than a very fast dilution.
To confirm this thesis different dilutions with inactive gas have been performed and the time lasted under low pressure conditions was recorded. The results of this experiment are shown in Figure 9.4.

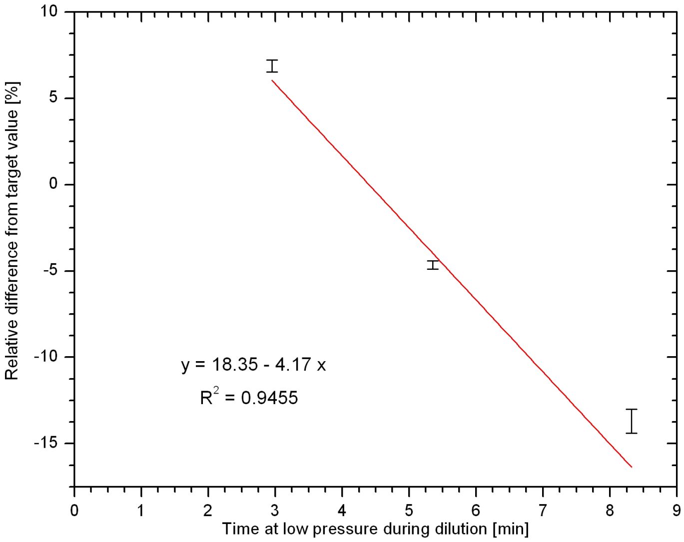

Figure 9.4: Inactive gas measurement for different dilution time.

For a theoretical dilution time of zero minutes, for which air contamination would have no influence, a concentration 18% greater than the target value should be measured. Based on these results it can be concluded that without air contamination the expected concentration should be measured.

9.4.2 Signal non-linearity

In the case of fission gases, Xe concentrations were computed using both isotope ratios (thus IDMS) and signal intensities. Ideally both method should lead to the same results although based on different calculations. However, it has been observed that the method based on signal intensity overestimates the concentrations from 2 to 5% (relative) compared to IDMS.
To investigate the reason for this difference the linearity of the signal intensity has been checked. Two mass-flow controllers have been used, one to control the

mass-flow rates of the spike (containing natural Xe at 20 ppm (n/n)) and the other one to control the mass-flow rate of the carrier, i.e. pure Ar. The sum of the two mass-flow rates has been kept constant at 25 mLn/min to not change the overall mass-flow rate in the plasma. Gradually the mass-flow rate of the spike has been increased from 0 to 25 mLn/min (and at the same time the one of the carrier reduced from 25 to 0 mLn/min). For every step the signal response has been measured and recorded. The result is shown in Figure 9.5.

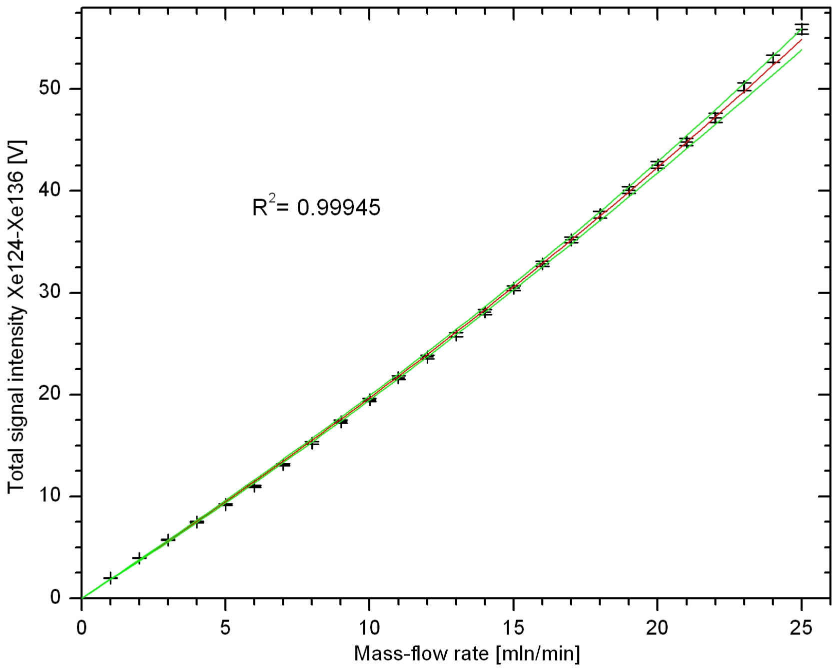

Figure 9.5: Non-linearity of signal intensities.

The signal intensity does not grow linearly with the mass-flow rate. In fact the best fitting has been obtained for the function given by:

$$y = y_0 + a \cdot \mathrm{e}^{b \cdot x} \tag{9.1}$$

where the coefficients are:

$$y_0 = -129.877 \qquad a = 129.888 \qquad b = 0.0141$$

This means that a doubled mass-flow rate does not correspond to a doubled signal intensity. Thus in the case of online gas measured, if spike and sample have the same concentration of Xe and the same mass-flow rates, the signal will not be doubled when the sample is added to the spike. With the curve obtained by fitting the data it has been found that using a method based on signal intensities Xe concentrations 2% grater than IDMS has to be expected.

Taking into account the result's relative uncertainty for the Xe concentrations obtained with both signal intensity method (from 1 to 2%) and IDMS (about 1%),

the differences between both methods can be better understood.
Furthermore, it was investigated if this non-linearity has also an influence on isotope ratio measurements. Figure 9.6 shows that isotope ratios change only slightly when the mass-flow rate of Xe in the MC-ICP-MS is changed.

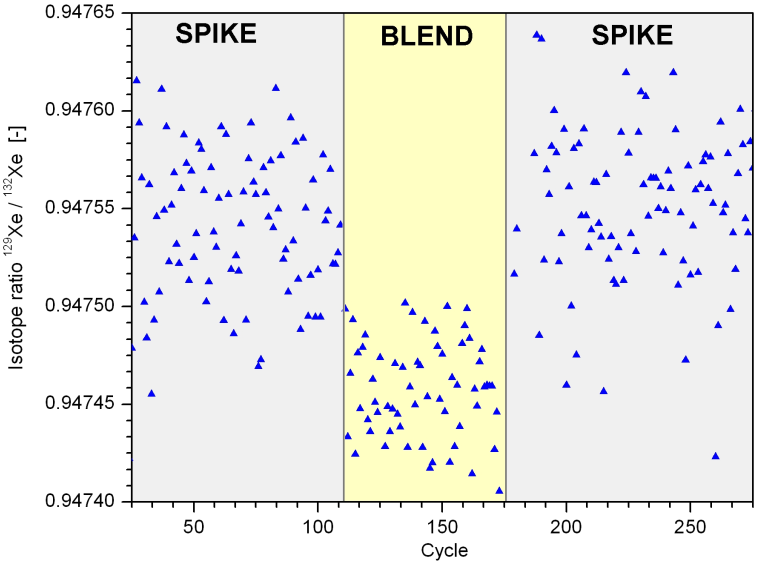

Figure 9.6: Change of a Xe isotope ratio during online measurements.

The difference observed in the isotope ratio when the sample is added to the spike is negligible compared to the overall relative uncertainty of the measurement in this study in the order of 1%.

9.5 MDD version 2.0

To solve the leak problems of the first version of the MDD all the valves previously used have been replaced. Diaphragm valves of Swagelok were chosen to substitute the ball valves. Diaphragm valves are especially designed to work under high vacuum condition (the manufacturer guarantees a leak rate of 10^{-9} mbar L^{-1} s^{-1}) and do not have a dead volume. A schematic and an image of a diaphragm valve are given in Figure 9.7.
To improve the repeatability of the dilution, pneumatic actuated valves were chosen. Because of this choice the design had to be slightly changed compared to version 1.2, since pneumatic valves does not allow partial opening and thus pressure cannot be gradually increased. A schematic of the design of the MDD version 2.0 is given in Figure 9.8, while a photo is given in Figure 9.9.
To introduce the sample in the device a system of two valves placed one after each other has been used. The procedure to introduce the sample is the following: before opening the manual throttle valve on the sample cylinder, the two valves on

the vacuum gauge (E and F) are closed. Later the valve connecting the sample with the MDD (valve F) is opened for two seconds and then closed again. During this first step the sample gas flows in the small volume on the vacuum gauge (given in red in Figure 9.8) but does not enter in the main part of the device. As second step valve E is opened and the sample gas contained in the puffer volume enters in the MDD. Using the above described procedure a limited amount of sample can be introduced in the system using pneumatic valves.

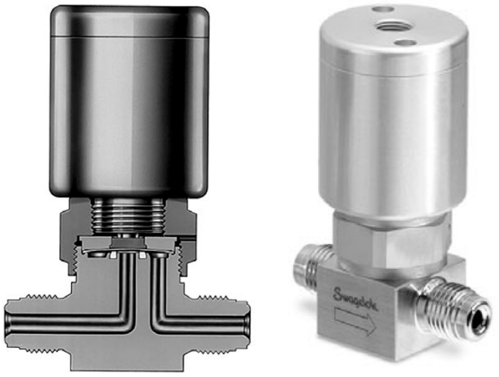

(a) Schematic. (b) Photo.

Figure 9.7: Diaphragm valve (Swagelok).

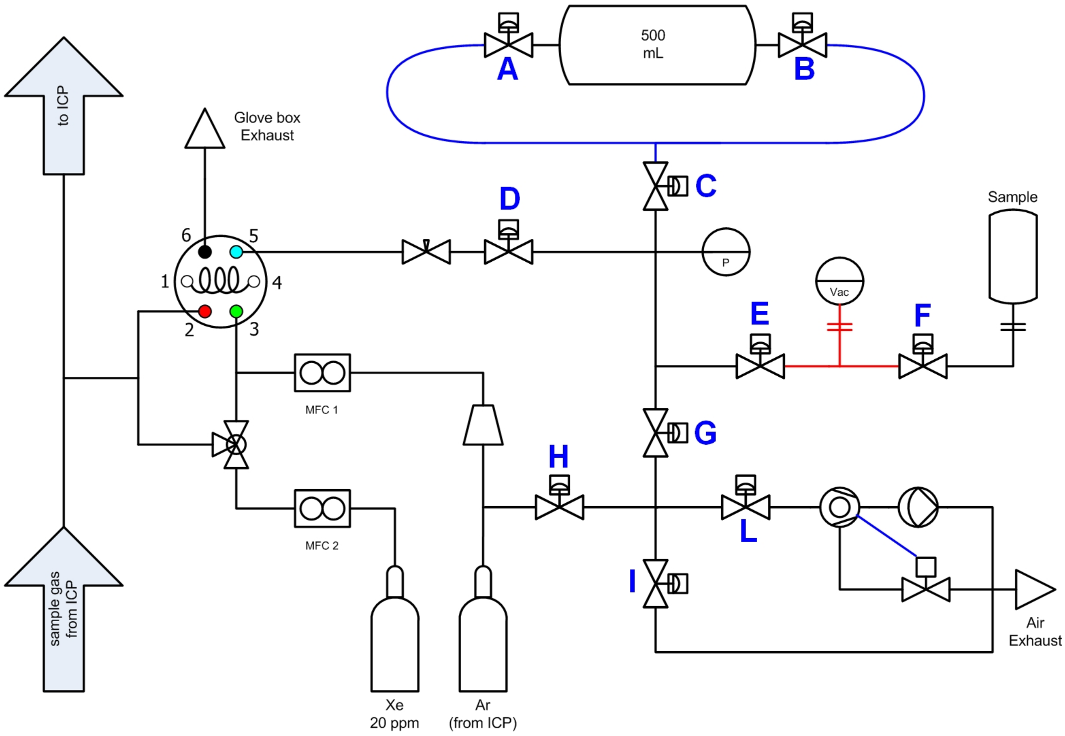

Figure 9.8: Mixing and diluting device, version 2.0.

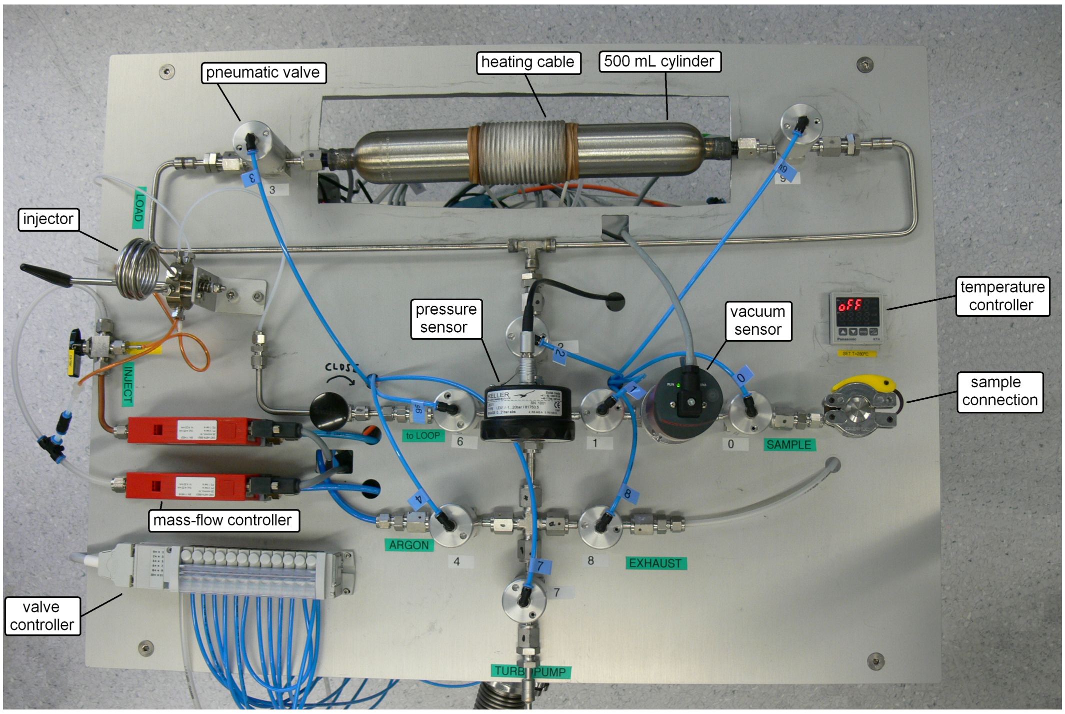

Figure 9.9: Top view of the mixing and dilution device, version 2.0. The molecular turbopump is located under the metal plate.

To further reduce the leak rate, VCR connections (Vacuum Coupling Radiation) were used to join the different components of the device (in the MDD version one Swagelok connections were used). VCR connections have the advantage of being designed for high vacuum condition and can be easily disconnected in case of design changes, unlike weldings. The combination of VCR connections and diaphragm valves has reduced the leak rate from 0.0003 mbar L^{-1} s^{-1} for MDD version 1.2 to less than 10^{-8} mbar L^{-1} s^{-1} for MDD version 2.0, i.e. of a factor of more than 10000.

After the encouraging results obtained heating the diluted sample in MDD version 1.2, a refined heating system has been built in MDD version 2.0. To heat the main cylinder an heating cable with a power of 490 W has been wrapped around the central part, leaving the extremities at free contact with air. This design was chosen to create temperature differences (and thus internal currents as for MDD version 1.2) and to avoid overheating of the valves placed at the endings of the cylinder. A thermocouple and a temperature controller were used to set and maintain temperatures in the order of 300°C in the central part of the cylinder. To accelerate the cooling down before the measurements, electric fans were placed on the top of the 500 mL cylinder.

A LabVIEW VI (Virtual Instrumentation) has been developed to control the valves and digitally read the values of the pressure sensor and the vacuum gauge using the computer (see Appendix A).

9.5.1 Dilution procedure

The dilution procedure adopted for version 2.0 is very similar to the one used in version 1.2, except the fact that the sample had to be introduced using an aperture sequence of valves, as described in the previous chapter.

At the beginning direct and indirect dilution procedures were adopted by using the gravimetrically determined volume ratio of 23.743. Later, however, using a pressure method, it has been found out that the volume ratio measured was not correct. Thus, to exclude the error given by the failure in the volume ratio determination only direct dilution was performed.

Because of the use of computer controlled pneumatic valves a recording of the valves position during the dilution can be obtained. Using the information stored, a valve diagram representing the position of each valve during the dilution can be obtained from the MATLAB code used for data post-processing (for details see Appendix B). An example of valve diagram is given in Figure 9.10.

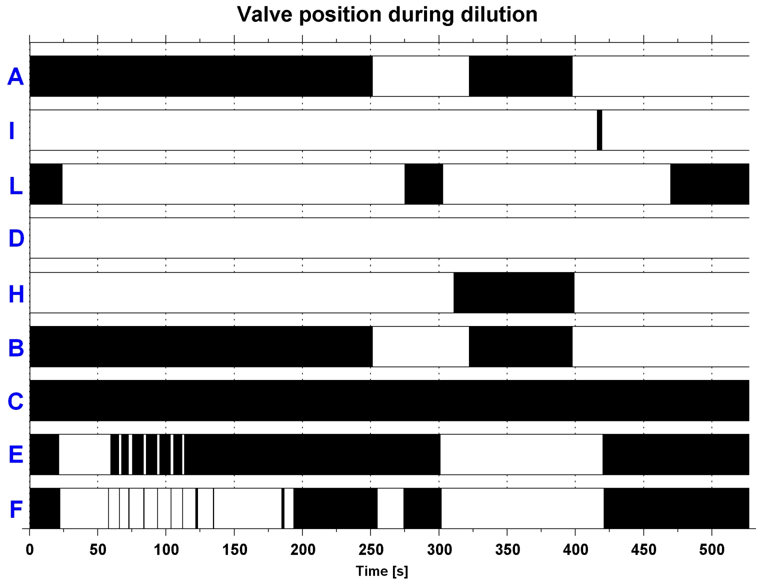

Figure 9.10: Valve diagram for the dilution of the sample FBA004-G4. Black lines indicate that the valve was open at the time given in the abscissa.

Using the LabVIEW software developed the dilution pressures can be chosen by the user. When a pressure is stored, automatically the standard deviation of the last n values (n can be choosen) is computed and later used for the measurement uncertainty calculation.

Because of the use of the computer to control the dilution, all the physical parameters influencing it can be recorded for a later analysis and uncertainties are readily computed. In addition, dilution procedures can be easily repeated and compared using the valve diagram.

9.5.2 Fission Xe measurements

Using MDD version 2.0 fission gases from a Swiss NPP have been diluted directly and measured. Each dilution has been homogenized for at least 100 minutes at 300°C. Measurements by MC-ICP-MS have been carried out using the online method and five or more injections have been performed for each dilution. Xe concentrations have been computed using the developed MATLAB post-processing code (see Appendix B) and the uncertainties using GUM (see Chapter 10). The results of GSMS and MC-ICP-MS are shown in Table 9.5.

Table 9.5: Xe concentration of fission gases measured with GSMS and MC-ICP-MS diluted using MDD version 2.0 (1*s* absolute uncertainties refer to method uncertainty).

Sample	MC-ICP-MS			GSMS	
FBA004-G4	DF [2]	Average	1*s*	Average	1*s*
Measurement 1	16964	31.84% (n/n)	0.36%	32.16% (n/n)	0.37%
Measurement 2	15589	32.42% (n/n)	0.37%	32.08% (n/n)	0.39%
Measurement 3	15554	31.97% (n/n)	0.36%	32.01% (n/n)	0.39%
Sample average	-	32.08% (n/n)	0.21%	32.08% (n/n)	0.22%

Sample	MC-ICP-MS			GSMS	
FBA004-B3	DF [2]	Average	1*s*	Average	1*s*
Measurement 1	14671	15.36% (n/n)	0.17%	14.98% (n/n)	0.19%
Measurement 2	17881	14.97% (n/n)	0.17%	14.95% (n/n)	0.19%
Measurement 3	25707	15.88% (n/n)	0.18%	14.74% (n/n)	0.20%
Sample average	-	15.40% (n/n)	0.10%	14.89% (n/n)	0.11%

Sample	MC-ICP-MS			GSMS	
FBA004-C2	DF [2]	Average	1*s*	Average	1*s*
Measurement 1	8936	22.79% (n/n)	0.26%	18.87% (n/n)	0.22%
Measurement 2	15139	23.52% (n/n)	0.27%	18.77% (n/n)	0.24%
Measurement 3	14038	23.40% (n/n)	0.26%	18.83% (n/n)	0.24%
Sample average	-	23.24% (n/n)	0.15%	18.82% (n/n)	0.14%

Sample	MC-ICP-MS			GSMS	
FBA004-D7	DF [2]	Average	1*s*	Average	1*s*
Measurement 1	17082	45.38% (n/n)	0.51%	36.80% (n/n)	0.41%
Measurement 2	14726	42.54% (n/n)	0.48%	36.76% (n/n)	0.43%
Measurement 3	11376	43.30% (n/n)	0.49%	36.65% (n/n)	0.44%
Sample average	-	43.74% (n/n)	0.29%	36.74% (n/n)	0.25%

---

[2] Dilution Factor

In the case of the sample FBA004-G4 a very good agreement is observed between the results obtained with MC-ICP-MS and GSMS. The measurements performed using GSMS show a very good repeatability with a sample relative uncertainty below 1%. Similarly the results obtained by MC-ICP-MS show a good repeatability and a sample relative uncertainty below 1%.

In the case of the sample FBA004-B3 a good agreement is observed between MC-ICP-MS and GSMS. It can be noticed that although very different dilution factors where applied, similar results were obtained in the three measurements. Similarly to the previous sample GSMS has a very good repeatability, with a relative uncertainty below 1%. The sample relative uncertainty for gas MC-ICP-MS is below 1% too. However, the standard deviation of the three measurements gives a relative deviation of almost 3%, suggesting that some uncertainty source has not been identified.

For the sample FBA004-C2 the same observations as for the previous samples for both GSMS and MC-ICP-MS concerning repeatability are valid. Again it is shown that although very different dilution factors were applied the results are very similar. In this case, however, there is no agreement between the results of GSMS and MC-ICP-MS. This is surprising, especially considering that the Xe concentration is similar to the one of sample FBA004-B3.

For the last sample measured, FBA004-D7, the same observations as for the last sample were made.

9.6 Conclusion on MDD version 2

The MDD version 2.0 has shown remarkable improvements compared to the MDD version one. Due to the reduced leak rate, time is no more an issue during the dilutions. In fact all the measured Xe concentrations are higher than the values obtained by GSMS, excluding the possibility of air contamination. In addition for two samples a good agreement has been found with the results obtained by GSMS. However, for the two other samples a large difference was observed for the values obtained from both devices. A very preliminary analysis could exclude a concentration dependent relationship for the differences between both methods, although considerations about the origin explaining the differences in the results obtained can only be done with a larger amount of experimental data.

Chapter 10

Uncertainty consideration

For both GSMS and MC-ICP-MS only considerations on the uncertainty can be made; accuracy cannot be determined since no certified sample is available that can be measured by both GSMS and MC-ICP-MS. For this reason this chapter will be focused only on the methods used to compute the uncertainty of the results.

10.1 Uncertainty of MC-ICP-MS measurements

As described in Chapter 7, small subsamples of the diluted gas contained in the main cylinder are extracted using the injector and measured by MC-ICP-MS. For a single dilution several injections (usually between five and seven) are repeated. To check the dilution repeatability of the MDD, for a single fission gas sample, the dilution is independently repeated three times. This measuring procedure creates uncertainties different levels and for each level an uncertainty has to be accounted. A schematic of the uncertainties for a single sample measurement is given in Figure 10.1.

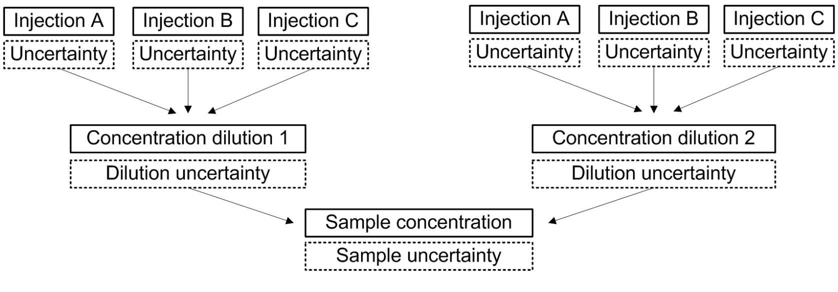

Figure 10.1: Measurement procedure for a single fission gas sample.

In a first step the uncertainties are computed using a MATLAB post-processing code (see Appendix B for a description and B.1 for an example of the output).

This code allows to calculate representative uncertainties for each experimental equipment in a very short time. Based on these uncertainties adjustments to the equipment used for the measurements (thus mass-flow controllers and MC-ICP-MS) can be made to reduce the measurement uncertainty. Typical parameters that can be tuned during the measurement are the mass-flow rate of spike and carrier and the ICP settings.
Later, using the data of several measurements, a unique method uncertainty has been computed using the GUM methodology (Guide to Expression of Uncertainty in Measurements [36]) in a more detailed manner.

10.1.1 Uncertainty calculation using MATLAB

Injection uncertainty

The Xe concentration in a single injection is computed using the IDMS equation. Since a dilution is performed, the standard IDMS equation (Equation 3.6) has to be multiplied by the dilution factor to obtain the original Xe concentration in the undiluted sample. The contribution of the different terms and their relationship in the IDMS equation is represented in Figure 10.2.

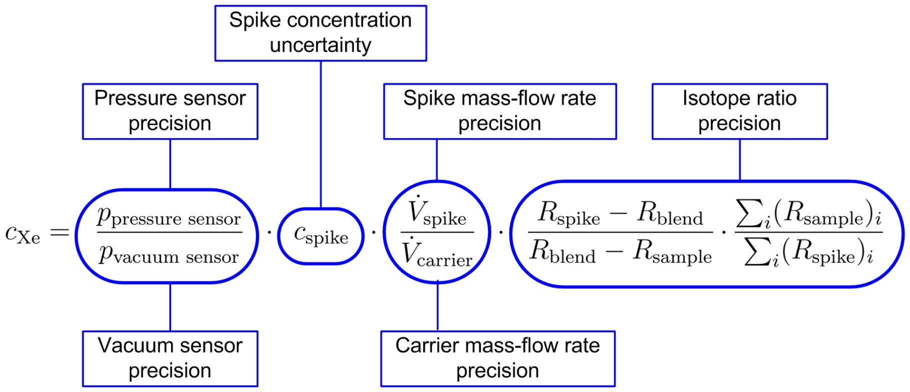

$$c_{\mathrm{Xe}} = \frac{p_{\text{pressure sensor}}}{p_{\text{vacuum sensor}}} \cdot c_{\text{spike}} \cdot \frac{\dot{V}_{\text{spike}}}{\dot{V}_{\text{carrier}}} \cdot \frac{R_{\text{spike}} - R_{\text{blend}}}{R_{\text{blend}} - R_{\text{sample}}} \cdot \frac{\sum_i (R_{\text{sample}})_i}{\sum_i (R_{\text{spike}})_i}$$

Figure 10.2: Uncertainties in IDMS equation.

The Xe concentration of the spike in the gas bottle is certified with a relative uncertainty of 0.5% ($1s$) from the manufacturer. The precisions of both the pressure and the vacuum sensor are computed using the standard deviation of the 30 values preceding the selection of the pressure by the user during the dilution process. The precision for each mass-flow controller is obtained from the standard deviation of the mass-flow rates (usually more than 500 values) recorded during the sample injection. Isotope ratio precisions for spike and blend are computed using the standard deviation of the recorded values.
The uncertainty of the Xe concentration computed using the IDMS equation is obtained by means of the classical method for uncertainty propagation. In general

for a function with argument A, B and C given by:

$$X = f(A, B, C, ...) \tag{10.1}$$

the propagated relative uncertainty is given by:

$$\sigma_{\mathrm{X}} = \sqrt{\left(\frac{\partial f}{\partial A}\sigma_{\mathrm{A}}\right)^2 + \left(\frac{\partial f}{\partial B}\sigma_{\mathrm{B}}\right)^2 + \left(\frac{\partial f}{\partial C}\sigma_{\mathrm{C}}\right)^2 + ...} \tag{10.2}$$

where σ_{A}, σ_{B} and σ_{C} are the relative uncertainties for the measured quantities A, B and C.
The modified IDMS equation (given in Figure 10.2) can be expressed as a function given by:

$$c_{\mathrm{Xe}} = f\left(\frac{p_{\text{pressure sensor}}}{p_{\text{vacuum sensor}}}, c_{\mathrm{spike}}, \dot{V}_{\mathrm{spike}}, \dot{V}_{\mathrm{carrier}}, R_{\mathrm{spike}}, R_{\mathrm{blend}}, R_{\mathrm{sample}}\right) \tag{10.3}$$

where $\frac{p_{\text{pressure sensor}}}{p_{\text{vacuum sensor}}}$ is the dilution factor. The expression of the uncertainty of the Xe concentration can be obtained by applying to the above form of the IDMS equation the simple rule of uncertainty propagation. However, because of the summations contained in the IDMS equation and the fact that R_{sample} is not directly measured, but obtained after some computational steps, the derivative terms in Equation 10.2 are rather complicated to compute. For this reason the analytical expression for the Xe uncertainty has been obtained using Mathematica and is then integrated in the code used for the post-processing of the measurements.

Dilution and sample uncertainty

The concentration for a single dilution is calculated from the average value obtained for the different injections. Its corresponding uncertainty is computed using the classical uncertainty propagation.
If n injections are performed, the average concentration is given by:

$$\bar{c} = \frac{c_1 + c_2 + c_3 + ... + c_{\mathrm{n}}}{n} \tag{10.4}$$

where c_1, c_2, c_3, ... , c_{n} are the concentration of the single injections. Applying Equation 10.2 and introducing the relative uncertainties for each injection given by σ_1, σ_2, σ_3, ... , σ_{n}, the dilution relative propagated uncertainty σ_{c} can be expressed as:

$$\sigma_{\mathrm{c}} = \frac{\sqrt{{\sigma_1}^2 + {\sigma_2}^2 + {\sigma_3}^2 + ... + {\sigma_{\mathrm{n}}}^2}}{n} \tag{10.5}$$

The same method is applied to obtain the sample concentration and its uncertainty starting from the values obtained for each dilution.

10.1.2 Uncertainty calculation using GUM

The ISO (International Organization for Standardization) GUM is an internationally recognized method used to compute uncertainties of measurements. It is based on the classical principle of uncertainty propagation. However, special correlations and refinements are employed in addition to the classical Gaussian formalism. GUM is widely used in inorganic chemistry and is recognized from the European Commission.

Similarly to other methods GUM allow to consider unidentified influences on the measuring procedure and to compute a representative uncertainty proper of the method used. The uncertainty for the ID-MC-ICP-MS measurements of this study has been computed using the experimental data available. The Xe concentration relative uncertainty for a single dilution has been determined as 1.13%.

The dilution uncertainties have been combined using the equation described in the previous section (Chapter 10.1.1) to obtain the sample uncertainties.

In addition, GUM has been used to compute the contribution of each single uncertainty to the uncertainty of the Xe concentration in fission gases diluted using the MDD and measured with ID-MC-ICP-MS. The results of this analysis are given in Figure 10.1.

Table 10.1: Single uncertainty contribution in MC-ICP-MS Xe concentration measurements (only contributions higher than 1% are displayed).

Certified spike concentration	25%
Blend measured ratio $\frac{^{129}\mathrm{Xe}}{^{132}\mathrm{Xe}}$	19%
Mass-flow controller spike	14%
Measured ratio $\frac{^{129}\mathrm{Xe}}{^{132}\mathrm{Xe}}$ in natural Xe	11%
Mass-flow controller carrier	11%
Pressure vacuum sensor	9.3%
Blend measured ratio $\frac{^{136}\mathrm{Xe}}{^{132}\mathrm{Xe}}$	5.8%
Blend measured ratio $\frac{^{134}\mathrm{Xe}}{^{132}\mathrm{Xe}}$	3.4%
Blend measured ratio $\frac{^{131}\mathrm{Xe}}{^{132}\mathrm{Xe}}$	1.4%

It can be observed that the largest contribution to the sample uncertainty is from the spike concentration. Unfortunately, this uncertainty cannot be reduced. In contrast the precisions of the mass-flow controllers for both spike and carrier can be reduced by limiting the pressure difference between entry and outlet. In general the isotope ratio precisions can be reduced by adjusting the mass-flow rate values to obtain the highest signal possible when the sample is introduced. However, it should be considered that by reducing the mass-flow rate, the precision of the mass-flow controller to which the change has been applied will decrease. On the other side increasing too much the mass-flow rate of the carrier will reduce the statistics available for the sample (the volume of the injector is fixed), thus influencing the precision of the ratios. It is therefore necessary to find an optimum between signal intensities and mass-flow rates. These considerations do not apply to the ratio $\frac{^{129}\mathrm{Xe}}{^{132}\mathrm{Xe}}$ which has been used as reference in the calculation of the spike abundance (see Chapter 3) and thus will have per definition higher uncertainty compared to other ratios.

10.2 Uncertainty of GSMS measurements

Measurements using GSMS are performed using the software provided by the manufacturer. The results of the measurements are given without uncertainties and no document is provided to explain the system which is used to calculate the data. The precision of the measurement performed by GSMS is obtained from the standard deviation of the measurements. In GSMS concentrations for the different elements in the fission gas are directly obtained as a result of the measurement, in contrast to ID-MC-ICP-MS where different calculations have to be performed. Thus the standard deviation of the concentration measured can be used directly as the precision for the concentration measurement. This precision is then combined with the uncertainties for the calibration bottles given in the certificates provided by the manufacturer.

In GSMS isotopic and elemental concentration of different element (like He and Kr) are used in the calculation of the concentration of Xe.

The contribution of single uncertainties to the Xe concentration uncertainty measured by GSMS computed using GUM is given in Table 10.2.

Table 10.2: Single uncertainty contributions in GSMS Xe concentration measurements (only contribution higher than 1% are displayed).

Certified He concentration calibration gas	33%
Xe concentration measured in fission gas	24%
Certified Xe concentration calibration gas	20%
He concentration measured in fission gas	9.6%
^{132}Xe abundance measured in fission gas	8.4%
Kr concentration measured in fission gas	2.1%
N_2 concentration measured in fission gas	1.3%
^{84}Kr abundance measured in fission gas	1.2%

In the case of GSMS the uncertainty cannot be further reduced by any mean, since it is mostly influenced by the quality of the calibration gas.

The measurements of fission gases in GSMS are performed in a very similar manner to MC-ICP-MS. In the case of GSMS it is not necessary to perform different injections, since the fission gas has not been treated before the measurement. Thus, for each sample three measurement are performed (corresponding to the three dilution per sample performed with MC-ICP-MS). The results obtained in the three measurement are combined using the same method used for MC-ICP-MS described in Chapter 10.1.1.

Part IV

Conclusions and outlook

Conclusions

An IDMS based method for the measurement of the Xe concentration in fission gases has been developed in the frame of this study. MC-ICP-MS has been used to perform the measurements of the Xe isotope ratios.

In order to successfully detect the isotopes of Xe without saturating the detectors of the MC-ICP-MS, fission gases had to be diluted up to concentrations in the ppm range. For this purpose a dedicated device has been built. Partial pressures of fission gases and Ar were measured to determine the dilution factor.

At the beginning of this study, experiments have been carried out with the prototype of the mixing and diluting device to check the capability of the device to repeatedly obtain homogeneous mixtures. The leak rate, the dead volumes and the geometry of the pipes and the cylinders used in the device have shown remarkable influence on the ability to achieve homogeneous mixtures. The use of an heater to enhance the internal mixing process before the measurements and the consideration of the Ar compressibility were other important aspects to be taken into account.

During the development phase, the original prototype has been almost completely changed concerning components and design, resulting in a final device capable of creating homogeneous mixtures of fission gases with a known dilution factor to be measured by MC-ICP-MS.

To perform the measurements of the fission gases by IDMS two mass-flow controllers and an injector were implemented. Certified natural Xe diluted in Ar at 20 ppm (n/n) has been used as spike. To compute the Xe concentration and obtain an estimate of the uncertainty, a post-processing code has been developed. The method uncertainty has finally been computed according to GUM.

Different fission gas samples have been diluted and measured using the hardware and the software developed and the results have been compared with the ones obtained by GSMS, assumed as reference method. The comparison of the results shows a non-consistency, ranging from very good agreement (less than 1% of relative difference) to considerable deviations (more than 20%). Nevertheless, because of the restricted set of data available for fission gas samples, the origin of these differences could not be identified so far.

Outlook

Considerable changes of the experimental equipment are not expected due to the high degree of optimization achieved in this study for the final design. However, small improvements to limit, for example, the Ar pressure (and thus the dilution factor) or to reduce the sample volume required for a measurement are realistic and realizable.

A large data set including measurements of fission gases with different Xe concentrations has be obtained to enable further investigations concerning the differences found in the results of MC-ICP-MS and GSMS. In this stage it will be important to measure gases with a wide range of Xe concentrations, from some percent up to 50% (n/n), to eventually identify concentration related trends.

During the measuring campaign other physical variables, in addition to the one considered in this study, which might influence the results (such as sample gas filling pressure, Ar maximum mass-flow rate, ICP settings...) should be taken into account to possibly find a relationship between them and the results obtained.

Appendix A

Control of MDD using LabVIEW

The flowchart for the control of the MDD version 2.0 performed using LabVIEW 2009 is shown in Figure A.1.

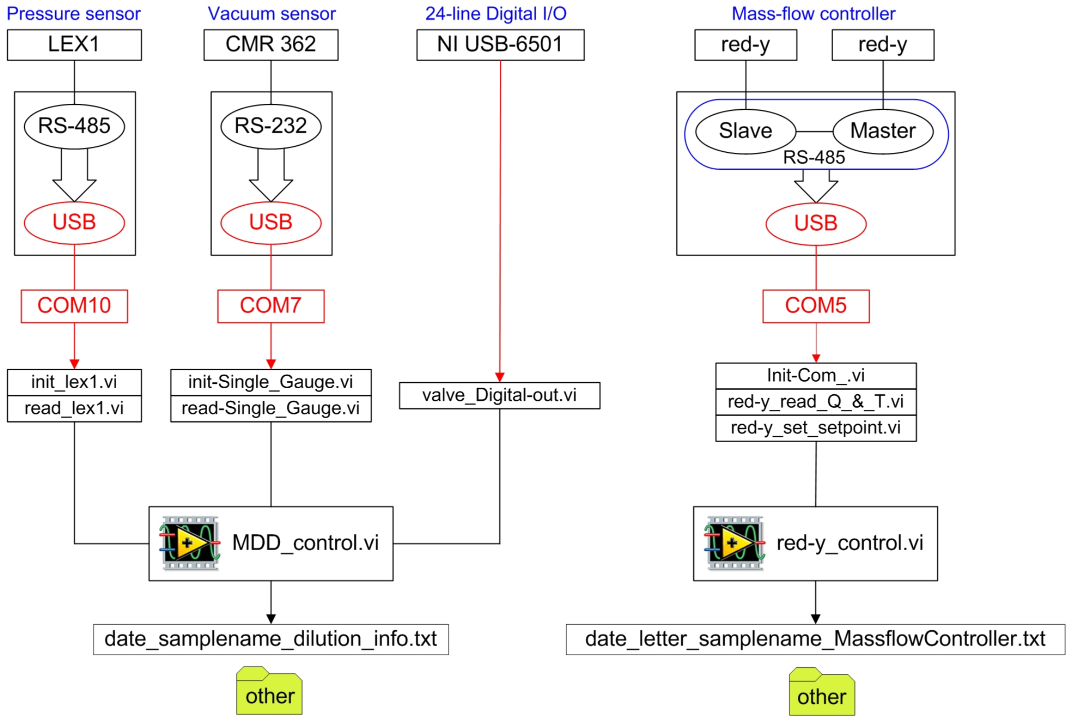

Figure A.1: LabVIEW MDD control flowchart.

To control the pneumatic valves of the device, the digital to analog converter NI-6501 of National Instruments has been employed. This device allows to generate logic TTL signals to be used to control the valves. A special electronic circuit has been build to use the low current 5 V TTL output signal to drive the 24 V current necessary to command the pneumatic switch system of the valves. The communication with the NI-6501 has been integrated in the VI (Virtual Instrumentation) *valve_Digital-out.vi* and has been performed using the direct USB connection between the computer and the device.

The RS-485 and RS-232 connections of the pressure and vacuum sensor have been converted into virtual COM port using an RS to USB converter. The conversion into USB allowed to connect different devices with different final connection by using a USB hub. In the dedicated VIs (*init_lex1.vi, read_lex1.vi, init-Single_Gauge.vi and read-Single_Gauge.vi*) both vacuum and pressure sensor are interrogated using standard COM communication procedures. In both cases two separated VIs were written to initialize the communication and to read the pressure (and the temperature in the case of the pressure sensor LEX1).

The three devices (pressure and vacuum sensor and the NI-6501) are constantly interrogated and updated from the main VI using the dedicated sub-VIs described previously. Valve position and the pressure of the LEX1 are read every 250 ms. The CMR 362 is read once a second.

When a dilution is performed a log can be created to record the valve position, the pressures and the temperature (obtained from the pressure sensor). The user can select both the low and high pressures that have to be used later to compute the dilution factor. The log file can be read using a dedicated MATLAB program to extract the most important information and visualize the pressures and the valve position during the dilution. As standard the log file should have a name given by the combination of data, sample name and the string *dilution_info.txt* and should be saved in the subdirectory *other* in the measurements main directory.

To read the values of the mass-flow controllers and set the set-values a separated VI has been developed. The communication system is similar to the one discussed for the pressure sensors. Slave and master mass-flow controller are connected each other using an RS-485 connection. With a RS to USB converter a virtual COM port is created allowing standard COM communication protocols on USB connection. The update frequency for the values from and to the mass-flow controllers can be manually set and reading up to 5 times a second can be reached.

During the measurement with MC-ICP-MS a log can be kept to check the capability of the mass-flow controller to maintain a constant mass-flow rate. The file containing the information should have a name composed by date, sample name, measurement letter and the string *Massflow_Controller.txt* in order to be correctly read from the dedicated MATLAB program.

A screenshot of the LabVIEW VIs is given in Figure A.2.

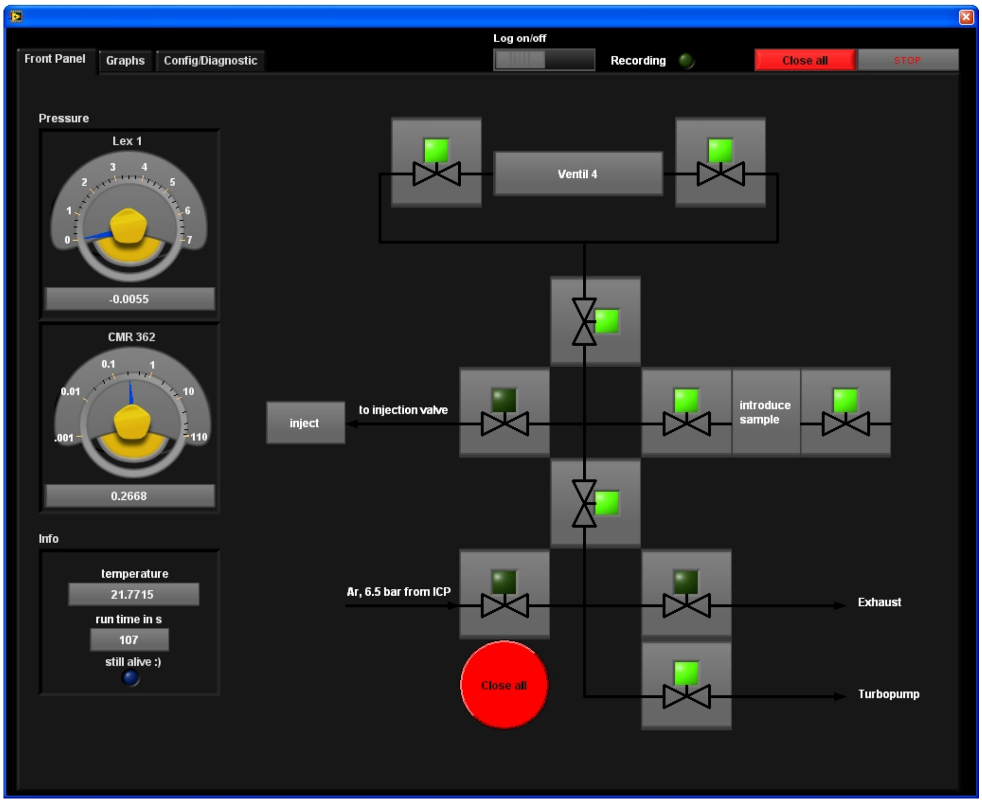

Lex 1: -0.0055

CMR 362: 0.2268

temperature: 21.7715

run time in s: 107

(a) Valve position and pressure readings.

COM port red-y: COM11

114516 [Carrier]

Setpoint [mln/min]: 0.00

Actual value [mln/min]: 0.0000

digital

Address: 2

Reading errors: 1

Temperature [°C]: 21.0060

114521 [Spike]

Setpoint [mln/min]: 0.00

Actual value [mln/min]: 0.0000

digital

Address: 1

Reading errors: 1

Temperature [°C]: 21.3128

Waiting time [ms]: 150

Timeout writing [ms]: 150

Timeout reading [ms]: 150

Runtime [s]: 23

Loop length [ms]: 224

Number of cycles: 103

Seperator: tab

Write interval: 5

Measurement name: noname A

(b) Mass-flow controller control.

Figure A.2: Screenshot of the LabVIEW VIs used to control the MDD version 2.0.

Appendix B

Calculation of Xe concentration using MATLAB

The flowchart of the MATLAB code written to calculate the Xe concentration in fission gases and its uncertainty is given in Figure B.1.

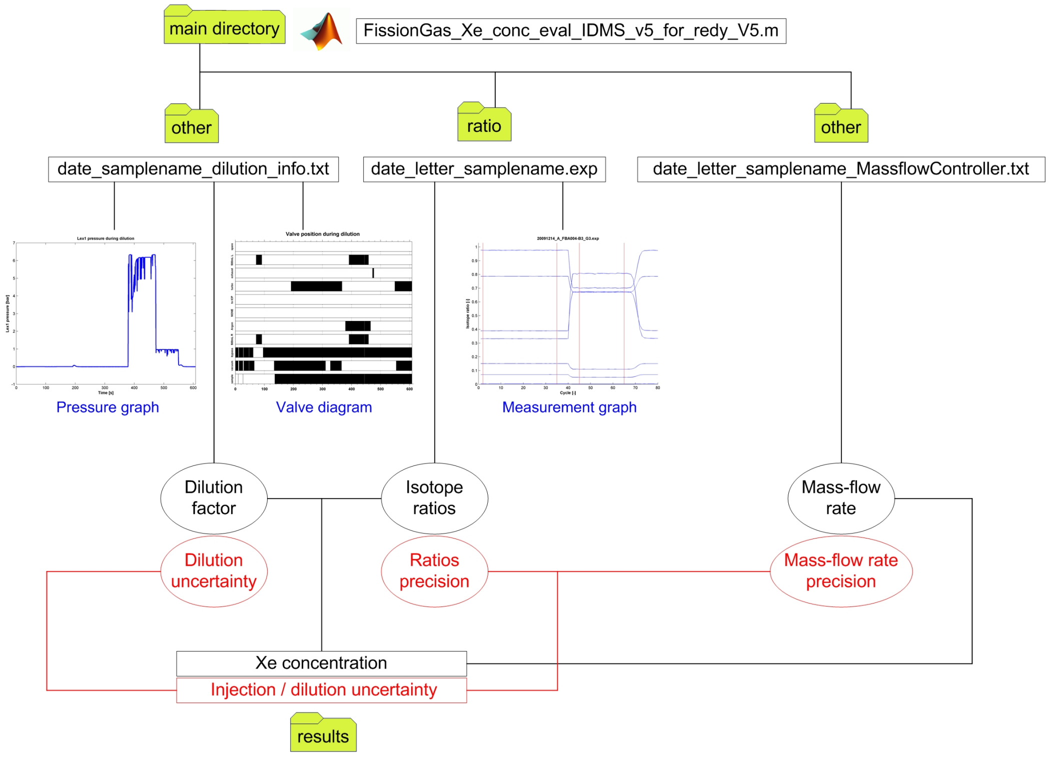

Figure B.1: Flowchart for the calculation of the Xe concentration using MATLAB.

The code, which has to be saved in the main directory of the measurement, retrieves the information concerning the dilution, the mass-flow rates of the gases during the measurements and the isotope ratios obtained by MC-ICP-MS from the log files and the raw files created by different separated software.

As discussed in Appendix A using the LabVIEW program for the control of the MDD device, there is the possibility to record a log during the dilution containing the most important physical variables. The MATLAB code automatically reads the low and high pressures that has been selected by the user during the dilution. The compressibility corrected dilution factor is easily computed by the ratio of the high and the low pressure. The precisions corresponding to the user selected pressures are computed using the standard deviation.

Once the information contained in the log file of the dilution are read, a graph of the pressures recorded by the CMR 362 and LEX1 sensor is automatically generated and saved. In addition, a bar diagram is created to visualize the position of each valve during the dilution.

With the software provided by Thermo Fisher Scientific to control the MC-ICP-MS there is the possibility to export the measured isotope ratios in an *.exp* file which can be easily read using different commercial programs such as Microsoft Excel. This *.exp* file, which has to be stored in the *ratio* subdirectory named with a combination of date, letter of the injection and sample name, is used to extract the isotope ratios of the blend and the spike. The user can choose between an auto mode, which automatically recognizes the region of blend and spike, and a manual mode, where the ranges have to be set manually. Precisions for every measurement are calculated using the standard deviation.

During each measurement with MC-ICP-MS a log file can be created by the dedicated LabVIEW program to store the mass-flow rates of spike and carrier. The log files are automatically read and the precision for each measurement is computed using the standard deviation.

With the quantities obtained from the different files, the sample Xe concentration is automatically computed with its corresponding relative uncertainty given for a preliminary estimate. All the graphs (pressures, valve position and isotope ratios) and a detailed report are stored in the *results* subdirectory. The report (saved as *.rtf* document) contains the isotopic composition of spike and sample, the diluted and original sample Xe concentration, the dilution factor, the low and high pressures selected during the dilution, the dilution temperature, the Ar compressibility and the mass-flow rates of both mass-flow controller. For each value the corresponding uncertainty (or precision) is given. An example of a report is given in Listing B.1.

The inputs required to run the program can be given in the first line of the code. The minimum requirement are the name of the sample, the date of the measurement and the letters corresponding to the injections that are to be evaluated. In addition it is possible to define fixed limits to determine the region of the spike and the blend (see Figure 7.3). In order to read the information from the files recorded during the measurement, the name of these files should follow the rules given in Figure B.1.

Listing B.1: Results report generated from the MATLAB code

```
--------------------------------------------------------------------------------
GLOBAL SUMMARY OF: 20091221_FBA004-G4_G2 INJECTIONS ABCDEFG
--------------------------------------------------------------------------------


-- ISOTOPIC COMPOSITION --

                        Spike                             Sample
Isotope         AVG (%)       ABS. UNC. (%)       AVG (%)      ABS. UNC. (%)
124Xe:         0.095385       0.000098           0.000033      0.002440
126Xe:         0.089173       0.000092           0.000031      0.002281
128Xe:         1.913002       0.001097           0.035770      0.003561
129Xe:        26.381060       0.008432           0.000000      0.000000
130Xe:         4.072037       0.001227           0.137813      0.006851
131Xe:        21.191461       0.003586           7.939379      0.028042
134Xe:        10.460102       0.003558          29.184047      0.076513
136Xe:         8.895972       0.005865          41.801019      0.144073
132Xe:        26.901807       0.001834          20.901908      0.018084


-- DILUTED SAMPLE Xe CONCENTRATION (n/n) --

18.7655 ppm (REL. UNC. 0.56401%)
Dilution uncertainty displayed (estimate)


-- ORIGINAL SAMPLE Xe CONCENTRATION (n/n) --

31.8354% (REL. UNC. 0.57324%)
Dilution uncertainty displayed (estimate)


-- ADDITIONAL INFORMATION --
Uncertainties and precisions displayed are relative

First pressure:             0.36662 mbar
Low pressure:               0.36662 mbar
Precision CMR 362:          0.27113%
Second pressure:            6.2002 bar
Precision Lex1:             0.00062902%
Volume ratio:               1 [-]
Dilution factor:            16964.8503 [-]
Dilution uncertainty:       0.0027113%
Compressibility Ar:         0.99688 [-]
Dilution temperature:       20.4258 [°C]
Precision MFC spike:        0.56144%
Temperature MFC spike:      23.3208 [°C]
Spike MFC mass-flow rate:   1.9993 [mln/min]
Precision MFC carrier:      0.25341%
Temperature MFC carrier:    23.0459 [°C]
Carrier MFC mass-flow rate: 2.0001 [mln/min]
Isotope ratios uncertainty: 1.1307% (estimate)
--------------------------------------------------------------------------------
FissionGas_Xe_concentration_IDMS_V.5.0
```

Bibliography

[1] M. Zimmermann, *Nuclear Fuels and Materials - Lecture's Slides*, EPFL, Autumn 2008

[2] H.-M. Prasser, *Nuclear Reactor Technology - Lecture's Slides*, EPFL, Autumn 2008

[3] INDC International Nuclear Data Committee, *IAEA Handbook of Nuclear Data for Safeguards*, INDC(NDS)-0534 Distr. SQ, 08.2008

[4] T.R. England, B.F. Rider, *Evaluation and Compilation of Fission Product Yields*, Los Alamos National Laboratory, October 1994

[5] E. A. C. Crouch, *Fission-Product Yields from Neutron-Induced Fission*, Atomic Data and Nuclear Data Tables, 19, 417-532, 1977

[6] S. Katkoff, *Fission-Product Yields from Neutron-Induced Fission*, Nucleonics, 18(11): 201-208, 1960

[7] D. Olander, *Fundamental Aspects of Nuclear Reactor Fuel Elements*, Office of Public Affairs, Energy Research and Development Administration, Oak Ridge Tennessee, 1976

[8] J. D. B. Lambert, R. Strain, *Oxide Fuels*, Argonne National Laboratory, Argonne, IL, USA

[9] C. Baker, *The fission gas bubble distribution in uranium dioxide from high temperature irradiated SGHWR fuel pins*, J. Nucl. Mater. 66, 1977, p. 283

[10] D. R. Lide, *CRC Handbook of Chemistry and Physics*, 1997

[11] *Atomic Weights of the Elements: Review 2000*, IUPAC Technical Report, Pure Appl. Chem., Vol. 75, No. 6, pp. 683-800, 2003

[12] Isotopen- und Elementanalytik OG 4325, *Analysenbericht 4898_ 4900*, PSI internal document, 07.2009

[13] *http://atom.kaeri.re.kr*, Pointwise ENDF-VI Library

[14] M. I. Horvath, *Development of a Method for Xenon Determination in the Microstructure of High Burn-up Nuclear Fuel*, Diss. ETH No. 17527

[15] M. Sargent, R. Harte, C. Harrington, *Guidelines for Achieving High Accuracy in Isotope Dilution Mass Spectrometry (IDMS)*, The Royal Society of Chemistry, 2002

[16] S. J. Hill, *Inductively Coupled Plasma Spectrometry and its Applications*, Blackwell Publishing, Second Edition, 2006

[17] S. Kashibe, K. Une, *Effect of Additives (Cr_2O_3, Al_2O_3, SiO_2, MgO) on Diffusional Release of ^{133}Xe from UO_2 fuels*, Journal of Nuclear Materials, 254, 234-242, 1998

[18] J. C. Killeen, *Fission Gas Release and Swelling in UO_2 Doped with Cr_2O_3*, Journal of Nuclear Materials, 88, 177-184, 1980

[19] *http://www.mtri3.eu*, Integrated Infrastructure Initiatives for Material Testing Reactor Innovations

[20] H. van der Merwe, J. Venter, *A Method to Evaluate Fission Gas Release During Irradiation Testing of Spherical Fuel*, Journal of Engineering for Gas Turbines and Power, 131, 2009

[21] V. Boutellier, H. Wiese, *Gasentnahme und Druckbestimmung an einem bestrahlten Brennstab*, PSI internal document, PL651_Gasentnahme

[22] J. S. Becker, *Inorganic Mass Spectrometry - Principles and Applications*, Wiley, 2007

[23] Balzers AG, *Betriebsanweisung Balzers GAM 442*, 1993

[24] B. Wernli, A. Hermann, *Bedienungsanleitung für das Gasmassenspektrometer GAM 442*, PSI technical report AW-43-98-02, 2005

[25] Thermo Electron Corporation, *Finnigan Neptune - Hardware Manual*, 2004

[26] E. Rosenberg, R. A. Hallama, M. Grasserbauer, *Development and Evaluation of a Calibration Gas Generator for the Analysis of Volatile Organic Compounds in Air Based on the Injection Method*, Fresenius Journal of Analytical Chemistry, 371, 798-805, 2001

[27] G. O. Nelson, *Gas Mixtures - Preparation and Control*, Lewis Publishers, 1992

[28] W. J. Baker, T. L. Zinn, *Preparation of gas calibration samples*, Perkin Elmer Instrument News, 11:1, 1960

[29] E. E. Hughes, W. D. Dorko, *Accurate Mass Spectroscopic Determination of Low Concentrations of Carbon Dioxide in Nitrogen*, Analytical Chemistry, 40:750, 1968

[30] J. Mettes, T. Kimura, M. Schack, *Apparatus for Producing Standard Gas Mixtures*, United States Patent Number: 5239856, 1993

[31] J. Mettes, T. Kimura, M. Schack, *Process for Producing Low-Concentration Gas Mixtures, and Apparatus for Producing the Same*, United States Patent Number: 5054309, 1991

[32] M. L. Malczewski, D. C. Heidermann, *System and Apparatus for Producing Primary Standard Gas Mixtures*, United States Patent Number: 7390346 B2, 2008

[33] W. J. Little, *Tables of Thermodynamic Properties of Argon from 100 to 3000 K*, Karman Gas Dynamic Facility, 1964

[34] E. L. Cussler, *Diffusion - Mass Transfer in Fluid Systems*, Cambridge University Press, Second Edition, 2003

[35] J. Hirschfelder, C. F. Curtiss, R. B. Bird, *Molecular Theory of Gases and Liquids*, New York: Wiley, 1954

[36] W. Bich, M. G. Cox, P. M. Harris, *Guide to the Expression of Uncertainty in Measurement*, Metrologia, 43, 161-166, 2006